Petroleum Science 20 (2023) 670–688

Contents lists available at ScienceDirect

Petroleum Science

journal homepage: www.keaipublishing.com/en/journals/petroleum-science

Original Paper

Hydrocarbon generation and organic matter enrichment of limestone in a lacustrine mixed sedimentary environment: A case study of the Jurassic Da'anzhai member in the central Sichuan Basin, SW China

Qi-Lu Xu [a, b], Bo Liu [b], Xin-Min Song [c], Qing-Ping Wang [a, *], Xu-Dong Chen [a], Yang Li [b, d], Yu Zhang [a]

[a] Shandong Provincial Key Laboratory of Deep Oil and Gas, China University of Petroleum (East China), Qingdao, Shandong, 266580, China
[b] Institute of Oil and Gas, Peking University, Beijing, 100871, China
[c] PetroChina Research Institute of Petroleum Exploration and Development, Beijing, 100083, China
[d] Petroleum Exploration and Production Research Institute, SINOPEC, Beijing, 100083, China

ARTICLE INFO

Article history:
Received 8 January 2022
Received in revised form
20 September 2022
Accepted 2 October 2022
Available online 6 October 2022

Edited by Jie Hao and Teng Zhu

Keywords:
Lacustrine limestone
Full-rock system
Organic matter evaluation
Paleoenvironments
Lake evolution
Terrestrial inputs

ABSTRACT

The hydrocarbon generation effectiveness of lacustrine limestone has been gradually proven. The Da'anzhai Member limestone is the most important Jurassic oil-producing layer in the central Sichuan Basin, and the characteristics of limestone organic matter are often overlooked. 175 typical samples of different lithologies from 19 wells were systematically analyzed to determine hydrocarbon generation, controlling factors and formation models by analyses of organic matter, minerals, elements, isotopes and petrography. (1) Lacustrine paleoenvironments can be beneficial for the enrichment of organic matter in limestone. A favorable environment would be a quiet, low-energy zone in a warm and humid climate with an appropriate supply of terrestrial inputs. (2) Lacustrine limestone has a higher organic matter conversion rate, and a lower hydrocarbon generation threshold than argillaceous source rocks, and can be effective source rock. (3) The mud-bearing shell limestone from the forebeach to the lake slope is thick, with a relatively high abundance of organic matter, and its hydrocarbon generation is effective. This study can clarify the effectiveness and enrichment of the limestone organic matters in the study area, and contribute to an understanding of hydrocarbon generation for full-rock system in a lacustrine mixed sedimentary environment.

1. Introduction

The effectiveness of marine carbonate source rocks has been widely confirmed, but research on lacustrine carbonate rocks is relatively lacking (Klemme and Ulmishek, 1991; Kietzmann et al., 2014; Koch et al., 2017; Luo et al., 2005; Hu et al., 2021; Lawal et al., 2021). Lacustrine carbonate source rock is different from mudstone or marine carbonate in many aspects, such as organic matter, hydrocarbon generation and mineral composition (Harris et al., 2004; Lima and DE Ros, 2019; Ke et al., 2022). The organic matters in carbonate and mudstone source rocks mainly come from the proteins and lipids of lower aquatic organisms, and the carbonate formation environment can also be suitable for high reproduction of these organisms (Harris et al., 2004; Lima and DE Ros, 2019; Xia et al., 2019). Marine carbonate rocks have relatively stable depositional thicknesses and scales. Under the guarantee of organic matter sources and preservation conditions, effective source rocks can be formed (Klemme and Ulmishek, 1991; Kietzmann et al., 2014; Koch et al., 2017; Luo et al., 2005; Hu et al., 2021; Lawal et al., 2021). Lakes have strong instabilities, and the sediment composition is often affected by the water system entering the lake in a mixed sedimentary environment (Wang et al., 1992; Lima and DE Ros, 2019). Compared with the marine sedimentary environment, the water area, depth, and volume of lakes are relatively low (Wang et al., 1992; Xue et al., 2007). Lakes lack environmental regulation capabilities and are susceptible to the impacts of the paleoenvironment and terrestrial inputs.

Many lacustrine carbonate source rocks have gradually been

* Corresponding author.
E-mail address: qingpwang@163.com (Q.-P. Wang).

https://doi.org/10.1016/j.petsci.2022.10.002

proven to be effective at generating hydrocarbons. Hydrocarbon generation and organic matter enrichment in lacustrine carbonate differ from those in marine carbonate. Effective lacustrine carbonate source rocks mainly include the Paleogene Shahejie Formation of the Dongpu Depression (Ke et al., 2022) and Jiyang Depression (Shi et al., 2020), the Cenozoic Formation of the Qaidam Basin (Guo et al., 2020), the Lower Cretaceous Toca Formation of the Congo Rift Valley (Harris et al., 2004), the Lower Cretaceous of the Brazilian Campos Basin (Stank et al., 1992), the Early Permian Fengcheng Formation of the northwestern Junggar Basin (Gao et al., 2018), the Paleogene Green River Formation of the Uinta Basin (Xia et al., 2019), and the Paleogene Western Qaidam Basin (Xing et al., 2022). During the deposition of lake basins, the surrounding rivers continuously carry detrital materials with abundant nutrients to the lake, which is conducive to the prosperity of a large number of lower aquatic organisms (Stank et al., 1992; Harris et al., 2004; Xia et al., 2019). Lacustrine carbonate organic matter also has the characteristics of multistage hydrocarbon generation and a high hydrocarbon conversion rate (Harris et al., 2004; Zhao et al., 2018). When the evaporation of the lake water is greater than the rainfall or the recharge of the river water, the lake water can be salinized, and the saline lake environment is conducive to the improvement of hydrocarbon production rate (Harris et al., 2004; Guo et al., 2020; Deaf et al., 2021). In addition, the hydrocarbon generation threshold of lacustrine carbonate source rocks is obviously lower than that of argillaceous source rocks. Fine-grained shale with TOC values greater than 0.4% can produce enough oil to support industrial accumulation, while for carbonate rocks, the minimum value can be as low as 0.3% or even 0.1% (Klemme and Ulmishek, 1991; Harris et al., 2004; Kietzmann et al., 2014; Gao et al., 2018; Xia et al., 2019). Lacustrine carbonate rocks, which have the ability to generate hydrocarbons, often coexist closely with lacustrine mudstone but are always ignored or treated as argillaceous source rocks. Many studies have shown that high-quality source rocks can be interbedded deposits of mudstone and carbonate rocks (Beckmann et al., 2005; Ruhl et al., 2010; Zhang et al., 2015; Zhou, 2018). For example, the effective carbon, hydrogen index, and degradation rate of the shale interbedded with limestone are greater than those of homogeneous shale in the 7th Member of the Triassic Yanchang Formation in the Ordos Basin, China (Zhou, 2018). This high-quality interbedded source rock also appears in the Cretaceous Campanian organic-matter-rich shale (Beckmann et al., 2005), the Early Jurassic Blue Lias Formation in southeastern England (Ruhl et al., 2010), and the Mesoproterozoic Xiamaling Formation in North China (Zhang et al., 2015).

The process of organic matter enrichment is complex, and the study of its laws can help clarify the process of hydrocarbon accumulation. Previous studies on organic matter enrichment were mainly based on mudstone. Research on whole-rock sections, including carbonate and mudstone, is relatively lacking. The controlling factors of organic matter enrichment in mudstone source rock have been widely explored in terms of preservation conditions, productivity, and dilution (Hao et al., 2011; Xu et al., 2017). Many factors have been confirmed, such as the salinity, redox and lake level (Hao et al., 2011; Xu et al., 2017; Qiu and He, 2021), properties of the sediment itself (size, weight, structure, etc.) (Shanks and Trent, 1980; Zonneveld et al., 2010), mineral composition (Kennedy et al., 2002), and microbial activity (Zhu and Jin, 2002). However, these control factors are basically aimed at the enrichment of organic matter in mudstone or marine environments, and the enrichment of lacustrine limestone has not been effectively studied.

Hydrocarbon generation by lacustrine carbonate rocks should play an important role in the oil supply to the Jurassic Da'anzhai Member in the central Sichuan Basin, SW China. The Da'anzhai Member is a typical limestone-mudstone deposit that formed in a lacustrine mixed sedimentary unit. It is the most important Jurassic oil-producing layer in the central Sichuan Basin and has yielded stable production for more than 60 years. It has cumulatively produced more than 500×10^4 t of crude oil and nearly 5×10^{10} m^3 of natural gas, accounting for 82% of the cumulative production of the Jurassic strata in the central Sichuan Basin (Chen et al., 2015; Yang et al., 2017). However, mudstone source rocks are characterized by a low abundance of organic matter, as evidenced by the TOC values from different research studies, including 0.16%–2.16% (Lu et al., 2014), 0.1%–2.2% (Xu et al., 2017), 1.5%–2% (Han et al., 2015) and 0.8%–1.7% (Jiang et al., 2016). The strong instability of the lake environment leads to impure lacustrine rocks that are mainly composed of interlayered mudstones and carbonate rocks. In this case, the cumulative thicknesses of mudstone reach 15–60 m, whereas those of limestone can reach 70–100 m (Zhang et al., 2013; Han et al., 2015). The maturity values of mudstone mainly range from 0.8% to 1.4% with an average of 1.1% (Han et al., 2015). Limestone samples with TOC values higher than 0.1% can reach 92%, and samples with TOC values higher than 0.25% can reach 60% (Zhang et al., 2013). The oil contribution of lacustrine limestone has been mentioned, but has not been systematically studied (Zhang et al., 2013; Han et al., 2015).

Based on the above, typical lacustrine limestone samples from the Da'anzhai Member were analyzed to determine the hydrocarbon generation, control factors and formation models. The effectiveness of limestone hydrocarbon generation is determined by organic matter evaluation. Organic matter enrichment in limestone is based on the paleoenvironment and sedimentary facies, as ascertained by petrology, mineralogy, wells, elements, carbon and oxygen isotopes, etc. The systematic study of lacustrine limestone source rocks can enrich the geochemical theory of terrestrial oil generation and contribute to an understanding of hydrocarbon generation for full-rock systems in a lacustrine mixed sedimentary environment.

2. Geological setting

The Sichuan Basin is located on the western margin of the Yangtze Platform and is a multicycle superimposed sedimentary basin in SW China. At the end of the Middle Triassic, the Indosinian movement caused seawater to withdraw from the Sichuan Basin; the basin entered the evolutionary stage of ring-shaped subsidence and began to receive terrestrial materials (Chen et al., 2015; Qiu et al., 2016; Yang et al., 2017).

The Jurassic Da'anzhai Member developed on the basis of silted lakes in the Ma'anshan Member and was deposited in a freshwater lake sedimentary system with a stable structural depression background in the Sichuan Basin (Fig. 1) (Di et al., 2013; Han et al., 2015). During this period, the lake transgression range was wide, and the water body was deep. The member is dominated by continental elastic rocks and carbonate rocks, and the thicknesses can reach 50–100 m (Lu et al., 2014; Chen et al., 2015; Yang et al., 2017). Therefore, this member has a large-scale and high-quality source-reservoir assemblage, yielding an important oil and gas production layer in the Jurassic strata of the Sichuan Basin (Deng et al., 2013; Yang et al., 2017).

Four sub-facies including semi-deep lake, shallow lake, shell beach and shore lake, occur sequentially from the center to the periphery of the lake basin, and the thickness has a ring-shaped distribution that tends to be thinner (Fig. 1) (Lu et al., 2014; Xu et al., 2020). The existence of a large number of freshwater paleontological organisms (lower protists, ostracods, pelecypods, charophytes, etc.) indicates a reducing environment with abundant water and rich nutrients (Fig. 2) (Han et al., 2015; Xu et al., 2019).

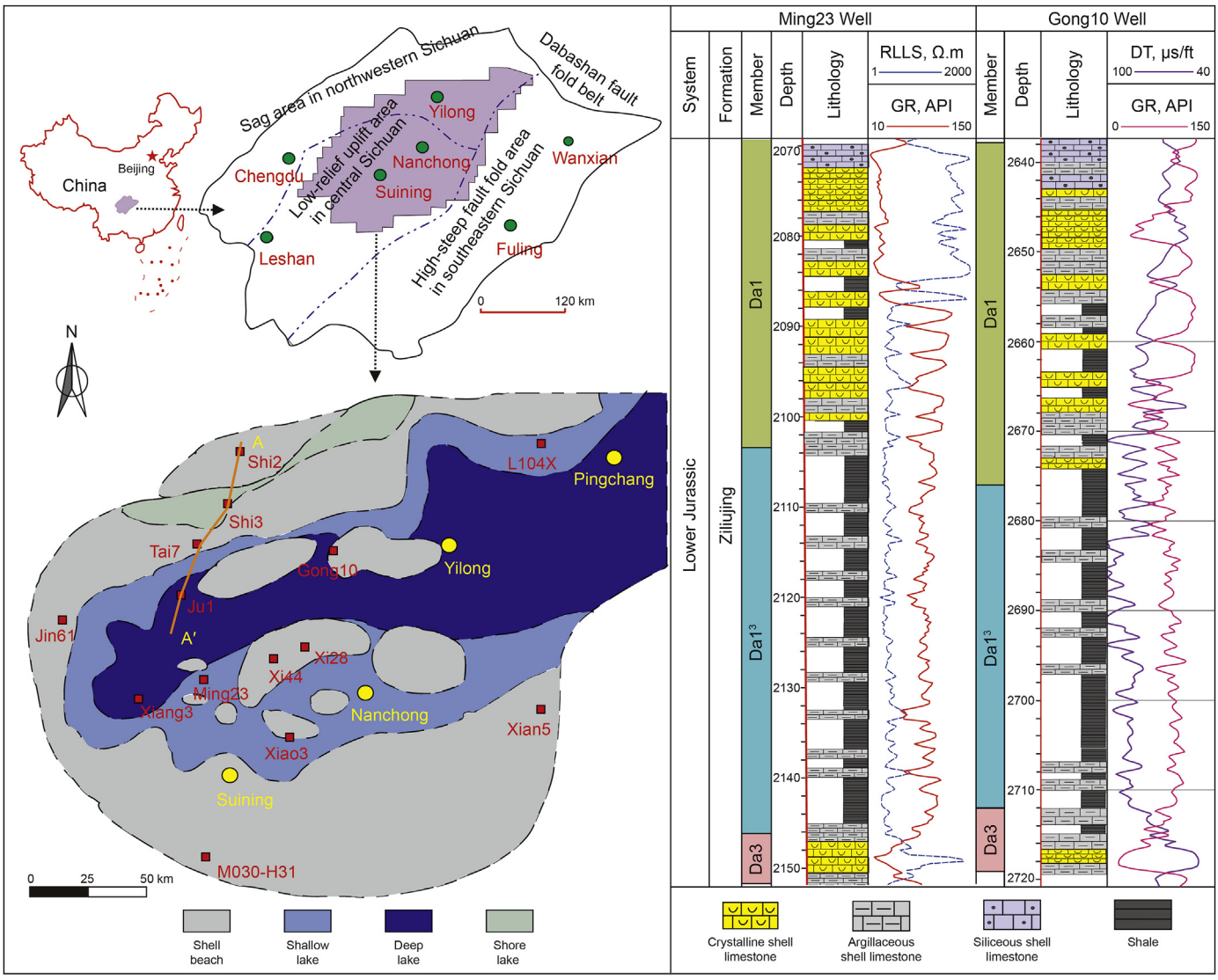

Fig. 1. Geological map and general stratigraphy of the Da'anzhai Member in the central Sichuan Basin.

It can be divided into the Da_3, Da_1^3 and Da_1 sub-members from bottom to top (Fig. 1) (Lu et al., 2014; Chen et al., 2015; Yang et al., 2017). The Da_3 sub-member is the product in the early stage of deposition, and the formation thickness is relatively thin, generally 5–14 m. The lithologies are mainly shell limestone, argillaceous shell limestone, and dark-grey shale. The Da_1^3 sub-member is a large set of dark shales intercalated with thin shell limestone, indicating a deep-water reducing environment. It has high deposition thickness and the organic matter content (Deng et al., 2013). The Da_1 sub-member is the sedimentary product of the uplift stage of the lake basin. The thicknesses are generally 30–45 m, and the lithology is mainly a large set of crystalline limestone and micrite shell limestone (Figs. 1 and 2) (Xu et al., 2017; Yang et al., 2017).

3. Samples and experimental methods

To analyze the hydrocarbon generation characteristics of the limestone, 175 samples of different lithologies from 19 wells in different sedimentary facies, including 113 limestone samples and 62 mudstone samples, were analyzed. The analytical tests included TOC analyses of 175 samples, Rock-Eval pyrolysis analyses of 148 samples, chloroform bitumen 'A' analyses of 64 samples, group component analyses of 38 samples, and vitrinite reflectance (R_o) values of 14 samples. The quantitative analyses of the effects of the paleoenvironment and sedimentary environment on limestone organic matter mainly included the major elements, trace elements, and carbon and oxygen isotopes.

Rock pyrolysis analysis was performed on samples with particle sizes of 0.07–0.15 mm with the Rock-Eval 6 instrument at the PetroChina Research Institute of Petroleum Exploration and Development. It mainly yielded T_{max}, S_0, S_1, S_2 and some derived parameters. Chloroform bitumen 'A' analysis is based on the content of organic matter dissolved in chloroform from solid samples by a mass method, and the weight was calculated at the China University of Petroleum (Beijing) and the PetroChina Research Institute of Petroleum Exploration and Development.

The major element samples were analyzed by X-ray fluorescence (XRF) spectrometry with an Advant' XP + analyzer at the School of Earth and Space Sciences, Peking University. The trace element data were obtained at the Beijing Research Institute of Uranium Geology using inductively coupled plasma-mass spectrometry (ICP-MS) following the standard of Pinto et al. (2012).

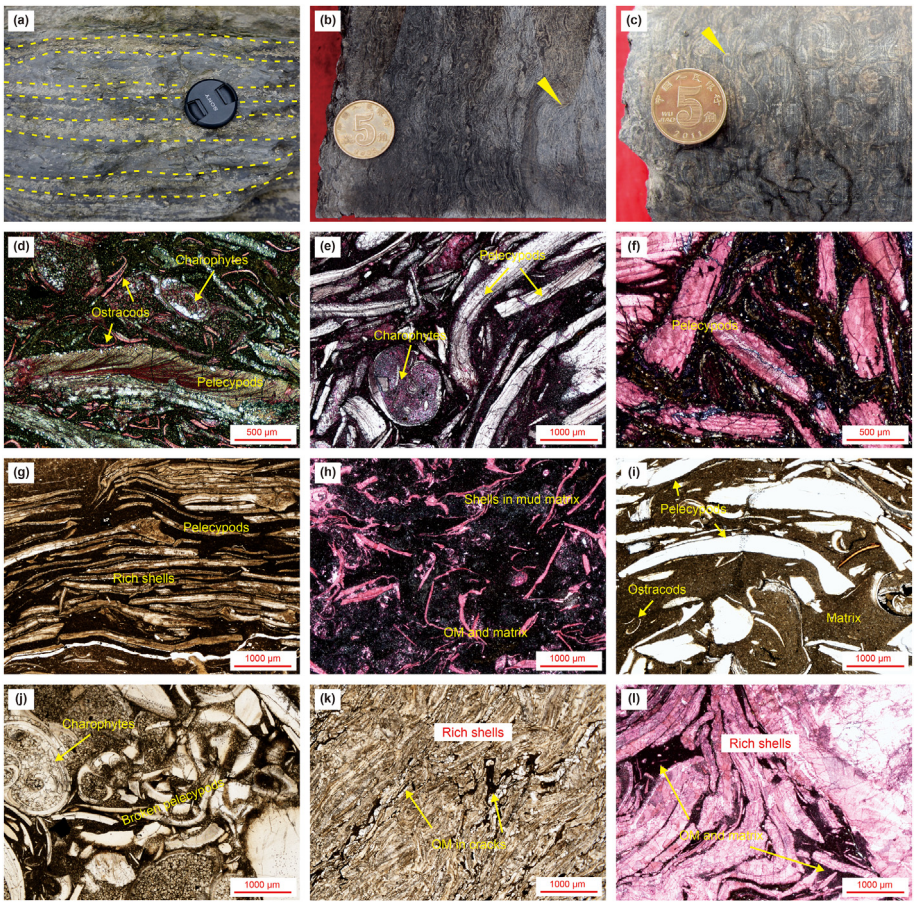

Fig. 2. Lacustrine limestones in the Da'anzhai Member of the central Sichuan Basin.
(a) Shell layers can be observed in the limestone of the Daluzhen field profile. (b) A large number of shells are visible in the shell limestone (X28, 1970.2 m). (c) A large number of shells are visible in the shell limestone (J61, 2679.5 m). (d) Various shells constitute the main frame of the limestone (X28, 1970.2 m). (e) Rich shells. A black matrix with organic matter is visible between the shells (W8, 2075.7 m). (f) Rich shells. A black matrix with organic matter is visible between the shells (Ju1, 2662.1 m). (g) Mud-bearing shell limestone. The rich shells constitute the main body of the limestone. The directional arrangement of the shell shows strong compaction (LQ104X, 3574.1 m). (h) Argillaceous shell limestone with rich organic matter. Shells are dispersed in the dark argillaceous matrix (MH31, 1416.45 m). (i) Argillaceous shell limestone. Shells are dispersed in the brown matrix with a relatively low organic matter content (G6, 2511.0 m). (j) Micrite shell limestone. Multiple shell types and broken pelecypods can be observed (Ju1, 2647.6 m). (k) Crystalline shell limestone. A small amount of organic matter is visible in the crack (W8, 2101.1 m). (l) Crystalline shell limestone (sparite shell limestone). The area where crystals develop has little organic matter and matrix (W8, 2080.9 m).

Powder samples react in phosphoric acid to form CO_2. Subsequently, the $\delta^{13}C$ and $\delta^{18}O$ concentrations of the CO_2 were analyzed on an IsoPrime 100 instrument at the School of Archaeology and Museology, Peking University. The isotopic analysis results were performed using the Pee Dee Belemnite (PDB) standard.

Analyses of the lithology, minerals, organic matter, and sedimentary environment were also based on various qualitative microscopic observations. General optical microscopy analysis and field emission scanning electron microscopy (FE-SEM) were completed at Peking University. An INCA Synergy system at the Key Laboratory of Orogenic Belts and Crustal Evolution was used to analyze the microstructure of each sample via FE-SEM and the mineral composition of each sample via energy dispersive spectroscopy (EDS). Some samples were subjected to argon-ion polishing to obtain higher resolution images. Fluorescence microscopy analysis was used to determine the presence of microscopic oily organic matter, and the experiment was conducted at the China University of Geosciences (Beijing).

4. Results

4.1. Hydrocarbon generation parameters of lacustrine limestone

Lacustrine limestone, especially argillaceous shell limestone interlayered with mudstone, has an obvious hydrocarbon generation effect. The TOC values of the limestone can reach 1.5%, and the average value is 0.3%. The average TOC of the argillaceous shell limestone even reaches 0.49%, and samples with TOC values exceeding 0.3% account for 57% of the samples (Fig. 3). The overall average value of chloroform bitumen 'A' in the limestone can reach 0.145%, and the total hydrocarbons (HC) can reach 559.5 μg/g (Fig. 3 and Table 1). The hydrogen index (HI) of limestone can reach 99.26 mg/g (9.09–282.76 mg/g). Although these parameters are lower than those of mudstone source rocks, they can still indicate good hydrocarbon generation for the limestone (Table 1).

Parameters, including 'A'/TOC, HC/TOC and the oil production index (OPI), accurately reflect the conversion rate of the original

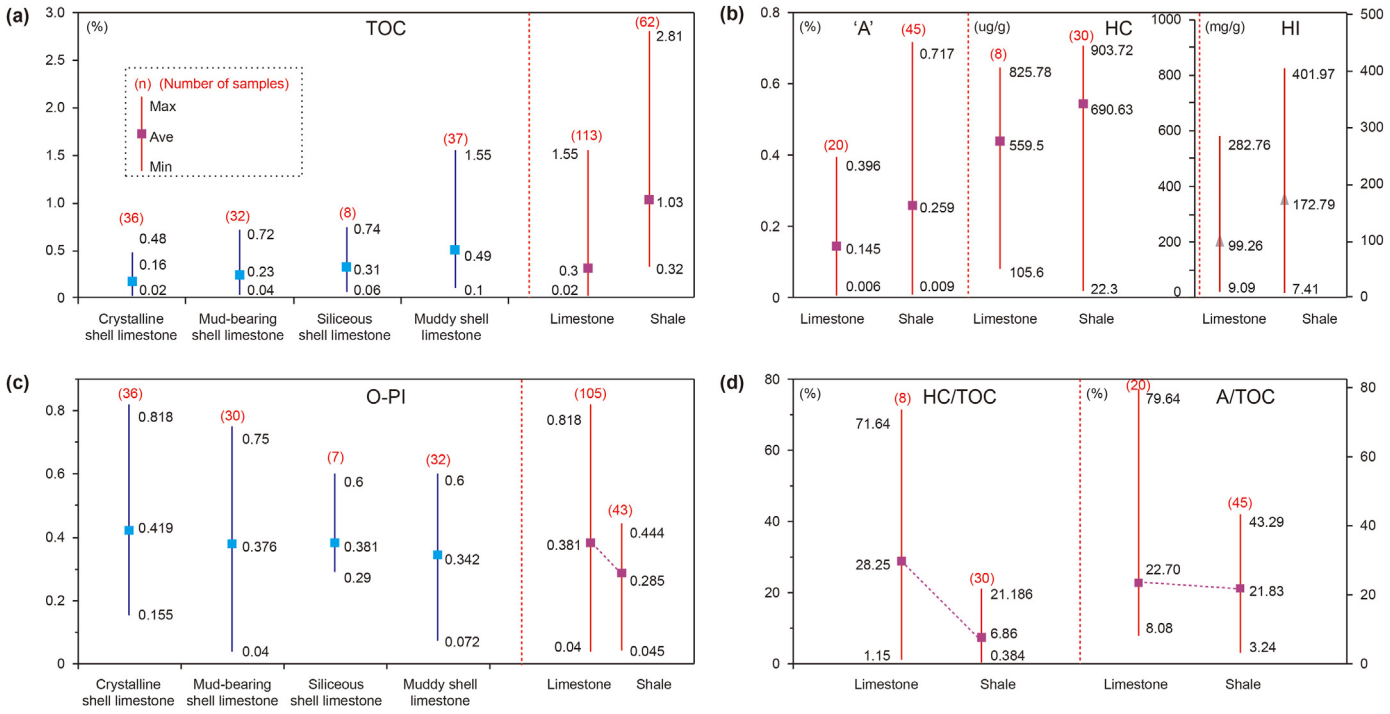

Fig. 3. Parameters of hydrocarbon generation for the lacustrine limestone.

organic matter (Fig. 3 and Table 1). (1) The average 'A'/TOC values of the limestone samples can reach 23.37%, and the average value for the mudstone samples is 22.92%. (2) The average HC/TOC values of the limestone samples can reach 28.25%, and the average value of the mudstone samples is only 6.86%. (3) The average OPI of the limestone samples was 0.381, and the average value of the mudstone samples is 0.285 (Fig. 3).

4.2. Paleoenvironment parameters of lacustrine limestone

4.2.1. Carbon and oxygen isotopes

The determination of carbon and oxygen isotopes in the initial sedimentary environment must be based on the evaluation of the diagenesis degree. Initially, the isotope samples were selected by observation with polarized light microscopy and cathodoluminescence microscopy. Micritic limestone with weak diagenesis or carbonate cement representing the original water environment can be favorable samples. In addition, Mn/Sr is a commonly used criterion for determining the diagenesis degree. Samples with Mn/Sr values > 2 poorly represent water body information (Kaufman et al., 1993). Most of the samples in the study area met the Mn/Sr criteria, but some samples do not (Table 2).

The average $\delta^{13}C_{PDB}$ of limestone in the study area is 3.38‰, with a range from 0.41‰ to 6.37‰. These values have the characteristic of obvious positive drift. The $\delta^{18}O_{PDB}$ values range from −13.56‰ to −7.28‰, with an average of −10.53‰. These values have the characteristic of obvious negative drift (Table 2). When the terrestrial oxygen isotope negative value is high, the carbon isotope positive value can also be high in lakes, while the marine sedimentary background is difficult to determine (Talbot, 1990, 1994; Zhang et al., 2013). When using the oxygen isotope value to determine the diagenesis degree, it is necessary to determine the oxygen isotope range of the entire layer and the background value range (Talbot, 1990, 1994; Zhang et al., 2013). All oxygen isotope values in the study area are negative, indicating that the background value is negative. Oxygen isotopes in the study area are not suitable for use in the determination of the diagenesis degree.

In a lake with open hydrological conditions, the renewal speed of the lake water is fast, and the residence time is short. Its carbon and oxygen isotope values typically indicate the isotope characteristics of injected water. In a long-term closed lake system, as evaporation increases, lighter carbon and oxygen isotopes preferentially escape, resulting in a relative increase in heavy isotopes and a simultaneous change of carbon-oxygen isotope values (Talbot, 1990, 1994; Zhang et al., 2013). It can be seen that the high negative oxygen isotope values in the study area can indicate the open lake basin type. The R^2 between $\delta^{13}C_{PDB}$ and $\delta^{18}O_{PDB}$ for the target limestone is only 0.092‰, which is significantly less than 0.5 (Fig. 4). The low correlation validates the weak diagenesis degree and indicates an open lake type with complex terrestrial inputs and stable spillover points (Talbot, 1990, 1994; Zhang et al., 2013).

4.2.2. Major and trace elements

The results of the element enrichment factor (EF) results reveal that Ca, P, Mn, Fe, and Mg are relatively highly enriched, while Na, K, Mn, and Ti are relatively less enriched (Fig. 5a). The enrichment of Ca, Mn, P, and Fe in limestone is significantly higher than that in mudstone, while the enrichment of K and Na in mudstone is significantly higher than that in limestone (Fig. 5a). The concentration of K is higher than that of Na, indicating the presence of potassium feldspar. In addition, Al and Ti are effective terrestrial indicator elements and have a good correlation (0.963), which excludes the influence of biological effects on Al (Table 3). K, Na, Si, Ti, and Al have a strong positive correlation, indicating that K, Na, and Si are mainly derived from terrestrial inputs (Table 3). However, Ca and these terrestrial elements, including K, Na, Ti, Si, and Al, show an obvious negative correlation, indicating that Ca was mainly formed spontaneously in lake basins (Table 3). There is no obvious correlation between Mg and other elements, indicating a

Table 1
Data from chloroform bitumen 'A', HC, rock pyrolysis and TOC (partial data) analyses of the limestone and shale in the Da'anzhai Member.

NO.	Well	Depth, m	TOC, %	Chloroform bitumen'A', %	HC, μg/g	HC/TOC, %	'A'/TOC, %	S_1, mg/g	S_2, mg/g	S_3, mg/g	T_{max}, °C	HI, mg/g	Lithology
1	LX2	1713.8	1.17	0.274	723.04	6.18	23.41	0.290	1.092		441	93.29	Shale
2	LX2	1726.1	1.07	0.463	679.01	6.35	43.29	0.150	1.282		446	119.80	Shale
3	PC1	3184.9	0.14	0.112			79.64	0.020	0.050		459	35.71	Limestone
4	PC1	3239.2	1.55	0.309			19.93	1.370	1.690		458	109.03	Limestone
5	PC1	3258.6	0.61	0.112			18.28	0.112	0.263		448	43.18	Limestone
6	PC1	3206.3	0.65	0.128			19.63						Shale
7	PC1	3221.2	1.51	0.237			15.71	0.157	0.936		453	61.96	Shale
8	PL10	1976.5	0.20	0.025	613.24	30.66	12.40	0.060	0.250	0.380	445	125.00	Limestone
9	PL10	1992.5	0.37	0.063	763.14	20.63	17.03	0.210	0.700	0.270	449	189.19	Limestone
10	PL10	2031.8	0.50	0.068	825.78	16.52	13.66	0.190	0.340	0.360	452	68.00	Limestone
11	PL10	2034.7	0.29	0.047	792.64	27.33	16.28	0.180	0.280	0.240	453	96.55	Limestone
12	PL10	1985.2	1.08	0.219	805.41	7.46	20.28	0.980	2.390	0.360	447	221.30	Shale
13	PL10	1986.8	1.22	0.280	856.93	7.02	22.93	1.400	3.020	0.250	448	247.54	Shale
14	PL10	1988.6	0.91	0.220	815.31	8.96	24.13	1.020	2.000	0.250	447	219.78	Shale
15	PL10	1990.2	0.84	0.230	823.96	9.81	27.35	1.320	1.650	0.270	447	196.43	Shale
16	PL10	1992.0	1.13	0.311	903.72	8.00	27.55	1.650	2.710	0.270	445	239.82	Shale
17	PL10	1993.1	1.28	0.416	814.34	6.36	32.48	2.170	3.650	0.270	445	285.16	Shale
18	PL10	1995.0	2.54	0.717	794.41	3.13	28.21	3.650	10.210	0.300	449	401.97	Shale
19	PL10	1997.0	2.81	0.455	657.25	2.34	16.19	2.450	10.400	0.290	449	370.11	Shale
20	PL10	2000.3	1.51	0.486	803.58	5.32	32.17	2.600	4.120	0.330	445	272.85	Shale
21	PL10	2004.2	1.62	0.489	827.40	5.11	30.16	2.810	4.220	0.250	447	260.49	Shale
22	PL10	2006.3	1.40	0.433	840.56	6.00	30.90	2.260	3.580	0.290	446	255.71	Shale
23	PL10	2007.9	1.89	0.496	814.94	4.31	26.22	2.670	5.560	0.290	446	294.18	Shale
24	PL10	2009.3	1.42	0.352	833.65	5.87	24.76	1.930	3.140	0.290	448	221.13	Shale
25	PL10	2011.5	2.22	0.504	817.63	3.68	22.69	2.530	6.470	0.280	447	291.44	Shale
26	PL10	2013.3	0.81	0.093	798.33	9.86	11.45	0.480	1.050	0.270	446	129.63	Shale
27	PL10	2015.3	1.63	0.331	770.34	4.73	20.31	1.720	3.730	0.250	446	228.83	Shale
28	PL10	2018.3	0.91	0.082	771.78	8.48	8.96	0.310	0.810	0.270	454	89.01	Shale
29	PL10	2022.6	1.12	0.204	832.17	7.43	18.17	1.010	1.700	0.280	451	151.79	Shale
30	PL10	2024.3	0.77	0.086	813.54	10.57	11.22	0.240	0.310	0.320	446	40.26	Shale
31	PL10	2028.9	1.72	0.306	813.56	4.73	17.78	1.440	3.690	0.250	450	214.53	Shale
32	S2	2891.6	0.06	0.006			11.09	0.033	0.054		500	97.82	Limestone
33	S2	2849.9	1.18	0.275			23.27	0.140	1.323		444	112.14	Shale
34	S2	2889.0	0.18	0.031	381.36	21.19	17.13	0.040	0.130		453	72.22	Shale
35	W6	2056.9	0.77	0.236			30.64	0.560	1.370		439.000	177.97	Limestone
36	W6	2097.5	1.30	0.261			20.05						Limestone
37	W6	2112.4	0.55	0.071			12.87						Shale
38	X20	1915.2	1.56	0.297			19.06	0.165	2.123		443.000	136.08	Limestone
39	X20	1837.9	2.09	0.582	143.30	0.69	27.86						Shale
40	X20	1844.4	0.76	0.128	682.75	8.98	16.88	1.230	2.100		445	276.32	Shale
41	X20	1850.1	0.37	0.041	493.72	13.34	11.09	0.100	0.270		451	72.97	Shale
42	X20	1862.3	0.80	0.332	283.64	3.55	41.50	0.087	1.832		439	228.96	Shale
43	X20	1925.6	1.85	0.204	360.88	1.95	11.03						Shale
44	X44	2102.2	1.06	0.361			34.09						Limestone
45	X44	2089.4	0.53	0.128	740.10	13.96	24.15	0.068	0.547		445	103.28	Shale
46	X44	2093.0	1.15	0.397			34.52	0.087	1.832		439	159.28	Shale
47	X44	2127.2	0.52	0.090			17.38	0.082	0.497		456	95.56	Shale
48	X8	1735.5	0.05	0.012	250.00	46.30	21.85	0.130	0.050		352	92.59	Limestone
49	X8	1752.6	0.48	0.136	566.96	11.81	28.33	0.130	0.050		352	10.42	Limestone
50	X8	1797.9	0.92	0.254	105.63	1.15	27.55	1.020	2.000		447	217.39	Limestone
51	X8	1807.3	0.08	0.006	558.82	71.64	8.08	0.050	0.030		450	38.46	Limestone
52	X8	1812.7	0.03	0.006			20.65	0.010	0.010		450	32.26	Limestone
53	X8	1756.5	0.58	0.127	22.30	0.38	21.97	0.140	0.660		452	113.79	Shale
54	X8	1761.2	0.52	0.101			19.50	0.120	0.430		447	82.69	Shale
55	X8	1780.7	0.84	0.223			26.60	0.890	1.220		444	145.24	Shale
56	X8	1803.7	0.49	0.057			11.65	0.290	0.640		452	130.61	Shale
57	C2	1900.5	0.88	0.171			19.47						Shale
58	C2	1924.0	0.29	0.009			3.24						Shale
59	G4	2429.9	0.90	0.153			17.04						Limestone
60	G4	2385.3	0.40	0.018			4.38	0.007	0.022	0.163	461	5.55	Shale
61	G4	2395.8	0.88	0.255			28.92	0.004	0.142	1.034	439	16.14	Shale
62	G4	2405.7	1.43	0.415			29.02	0.225	0.711		428	49.69	Shale
63	G6	2573.7	0.85	0.204			23.95						Shale
64	J61	2698.1	1.49	0.396			26.58	0.165	2.123		443	142.48	Limestone
65	J61	2706.8	0.38	0.045			11.79	0.223	0.676		443	177.79	Limestone

complicated source of Mg (Table 3).

Except for the Sr content, the trace element content of mudstone is generally higher than that of limestone (Fig. 5b). Overall, the contents of Sr, Ba, Rb, and V are relatively high, while the contents of In and Cd are relatively low (Fig. 5b). The rare earth element (REE) contents of mudstone are significantly higher than those of limestone. There is obvious enrichment in light REEs (LREEs) and depletion in heavy REEs (HREEs) in both mudstone and limestone, and the HREE curves are relatively flat (Fig. 6). Among the REEs, the contents of La, Ce, and Pr are relatively high, and the contents of Tm, Yb, and Lu are relatively low. Eu has significant low-value characteristics, especially in mudstone (Fig. 6).

Table 2
Carbon and oxygen isotope values of the limestone and shale in the Da'anzhai Member.

NO.	Well	Depth, m	Lithology	$\delta^{13}C_{PDB}$, ‰	$\delta^{18}O_{PDB}$, ‰	Mn/Sr	NO.	Well	Depth, m	Lithology	$\delta^{13}C_{PDB}$, ‰	$\delta^{18}O_{PDB}$, ‰	Mn/Sr
1	G10	2650.75	Limestone	1.19	−10.08	8.16	33	LX2	1712.40	Mudstone	3.12	−9.77	0.29
2	G10	2700.70	Mudstone	3.97	−8.35	3.69	34	LX2	1726.10	Limestone	3.85	−11.02	0.91
3	G10	2714.60	Mudstone	3.24	−10.71	0.16	35	M23	2113.18	Limestone	2.92	−9.60	0.49
4	G3	2333.60	Limestone	3.30	−13.26	0.80	36	MH31	1400.70	Limestone	1.75	−11.41	6.58
5	G3	2356.90	Mudstone	5.41	−5.61	3.88	37	MH31	1400.89	Limestone	2.15	−11.00	0.07
6	G3	2398.50	Limestone	5.13	−12.68	0.51	38	MH31	1416.50	Limestone	3.83	−13.25	0.77
7	G4	2385.30	Mudstone	2.37	−8.62	9.36	39	MH31	1426.26	Limestone	3.67	−8.00	0.18
8	G4	2395.80	Mudstone	3.52	−7.95	0.74	40	PC1	3221.20	Mudstone	2.95	−12.79	1.45
9	G6	2509.40	Limestone	2.94	−8.59	0.05	41	PC1	3239.19	Mudstone	2.42	−12.68	2.73
10	G6	2524.99	Limestone	2.03	−12.49	1.79	42	PC1	3258.58	Mudstone	3.03	−12.47	1.43
11	G6	2525.08	Limestone	−2.45	−9.36	10.64	43	PC1	3215.89	Mudstone	0.62	−12.49	1.65
12	G6	2536.82	Limestone	2.99	−10.24	0.41	44	S2	2818.60	Limestone	2.31	−9.36	0.04
13	G6	2580.05	Limestone	4.23	−10.34	0.42	45	S2	2886.28	Limestone	5.50	−12.99	0.47
14	J45	2632.39	Limestone	3.19	−7.46	0.65	46	S2	2887.02	Limestone	6.08	−12.86	0.60
15	J45	2656.00	Limestone	2.38	−12.88	1.43	47	S2	2890.00	Limestone	−1.19	−12.74	6.56
16	J45	2676.23	Limestone	4.31	−10.68	0.82	48	X20	1844.40	Mudstone	2.62	−10.59	0.92
17	J53	2827.30	Mudstone	1.04	−8.94	3.26	49	X28	1960.06	Limestone	2.43	−9.65	0.19
18	J61	2664.35	Limestone	2.99	−13.56	0.31	50	X28	1983.57	Limestone	3.21	−7.99	0.18
19	J61	2667.56	Limestone	0.41	−9.97	0.75	51	X28	2025.65	Limestone	6.37	−13.28	0.44
20	J61	2670.20	Limestone	3.34	−12.03	0.09	52	X3	2232.80	Limestone	2.59	−9.36	0.76
21	J61	2701.95	Limestone	2.57	−7.47	0.49	53	X3	2274.55	Limestone	3.98	−7.28	0.16
22	J61	2704.70	Limestone	3.96	−8.06	0.17	54	X44	2074.80	Limestone	2.93	−10.93	0.52
23	J61	2706.53	Limestone	2.93	−10.33	2.32	55	X44	2081.54	Limestone	1.42	−5.46	2.18
24	J61	2706.80	Limestone	3.47	−12.27	0.61	56	X44	2093.00	Mudstone	2.79	−9.57	0.23
25	J61	2725.00	Limestone	2.86	−9.46	0.10	57	X44	2093.60	Limestone	3.36	−9.18	0.23
26	J61	2698.10	Limestone	3.08	−9.36	0.74	58	X44	2119.40	Limestone	3.68	−9.87	0.41
27	L104X	3498.58	Limestone	2.51	−11.32	1.29	59	X44	2130.36	Limestone	3.40	−9.11	0.27
28	L104X	3518.14	Limestone	1.83	−12.58	6.37	60	X44	2133.40	Limestone	3.06	−11.55	0.83
29	L104X	3528.75	Limestone	0.81	−13.95	5.94	61	X44	2135.45	Limestone	1.16	−8.04	2.08
30	L104X	3548.12	Limestone	4.24	−11.86	2.71	62	X44	2089.40	Mudstone	3.00	−9.78	1.35
31	L104X	3574.10	Limestone	4.46	−11.25	2.13	63	X8	1780.70	Mudstone	2.88	−10.46	0.28
32	L104X	3576.95	Limestone	4.40	−11.02	1.72	64	XIA3	1785.20	Limestone	2.96	−10.68	0.67

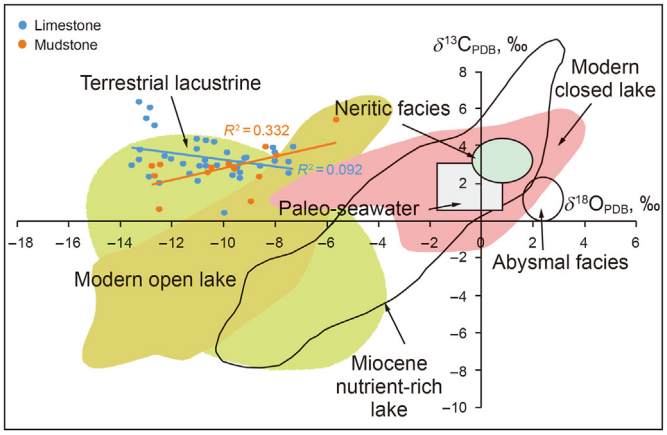

Fig. 4. Intersection diagram of $\delta^{13}C_{PDB}$ and $\delta^{18}O_{PDB}$ values showing the lake type (Veizer et al., 1999; Zachos et al., 2001; Zhang et al., 2013).

5. Discussions

5.1. Effectiveness of limestone hydrocarbon generation

Large amounts of sedimentary organisms and organic matter were observed in limestone from the Da'anzhai Member of the central Sichuan Basin (Figs. 2 and 7). Under microscopic observation, abundant fossils including ostracods, pelecypods, charophytes, and terrestrial plant fragments, were observed, indicating the rich accumulation of primitive organisms (Figs. 2 and 7).

Observing the fluorescent color, brightness and distribution of organic matter under a fluorescence microscope is a simple and reliable method for determining hydrocarbon generation in carbonate source rocks (Wang et al., 1992). Under a fluorescence microscope, large amounts of fluorescent materials were commonly observed in shell limestone, and they were generally located in the matrix between, around or in the shells (Fig. 7). FE-SEM observations showed abundant organic matters in the argillaceous shell

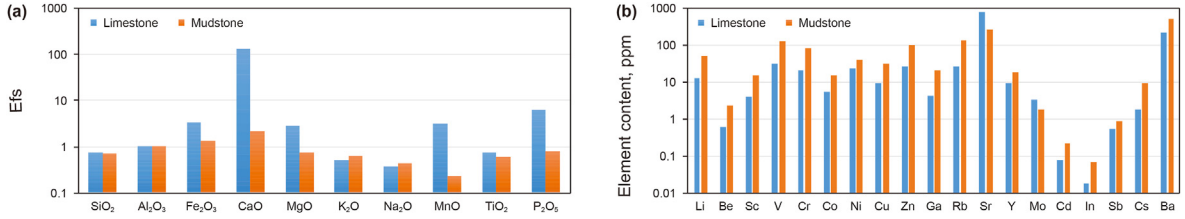

Fig. 5. Element enrichment characteristics. (a) EFs of major elements; EF = molar [(*i*/Al)sample/(*i*/Al)Average Shale], where *i* represents the element (Wedepohl, 1971; Ross and Bustin, 2009). (b) Distribution of the trace element content.

Table 3
Correlation coefficients of major element oxides.

	SiO_2	Al_2O_3	Fe_2O_3	CaO	MgO	K_2O	Na_2O	MnO	TiO_2	P_2O_5
SiO_2	1									
Al_2O_3	0.959	1								
Fe_2O_3	0.812	0.859	1							
CaO	−0.982	−0.984	−0.852	1						
MgO	0.288	0.301	0.320	−0.401	1					
K_2O	0.924	0.987	0.840	−0.962	0.322	1				
Na_2O	0.894	0.806	0.714	−0.851	0.222	0.755	1			
MnO	−0.141	−0.166	−0.032	0.142	−0.004	−0.179	−0.137	1		
TiO_2	0.962	0.963	0.829	−0.965	0.255	0.925	0.828	−0.143	1	
P_2O_5	−0.105	−0.084	0.023	0.117	−0.223	−0.119	−0.092	0.112	−0.021	1

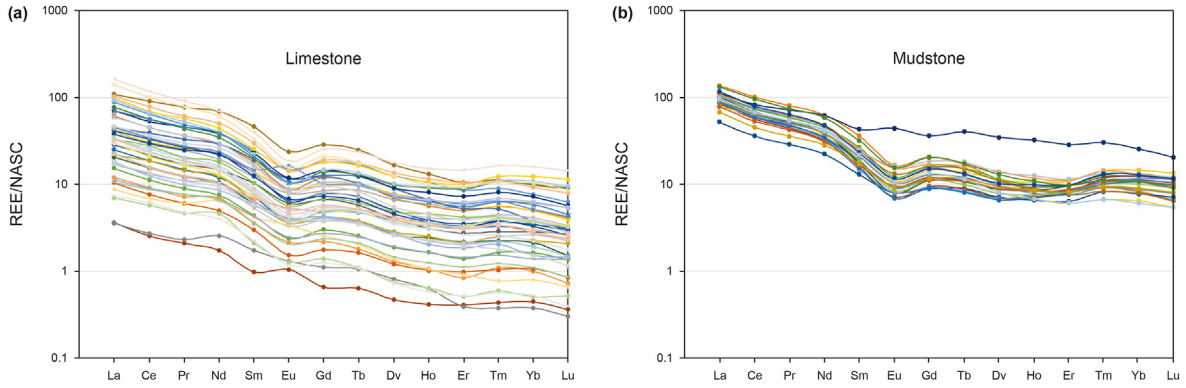

Fig. 6. Chondrite-normalized REE diagrams of limestone and mudstone in the Da'anzhai Member.

limestone (Fig. 7). In addition, abundant organic matter pores and in situ dissolution indicate that the organic matter underwent a strong hydrocarbon generation process (Fig. 7). In short, a large amount of original organic matter was present, and it underwent a strong hydrocarbon generation process (Liu et al., 2021).

Although the organic matter abundance of carbonate rocks was usually lower than that of mudstones (Fig. 3), the hydrocarbon generation of carbonate rocks can be effective for the following reasons.

1. The hydrocarbon generation threshold of lacustrine carbonate source rocks is obviously lower than that of argillaceous source rocks. Fine-grained shale with TOC values greater than 0.4% can produce enough oil to support industrial accumulation, while for carbonate rocks, the minimum value can be as low as 0.3% or even 0.1% (Table 4). In the carbonate source rock evaluation system, the organic matter abundance of the Da'anzhai limestone can be effective.

2. The conversion rate of organic matter in carbonate source rocks is usually higher than that in argillaceous source rocks. The organic components in carbonate rock are mainly composed of proteins and fatty compounds with a small amount of humus, while those in mudstone are mainly composed of insoluble organic matter such as humus. The conversion rate of organic matter dominated by proteins and fatty compounds is significantly higher than that of humus (Zhou and Jia, 1974). The 'A'/TOC, HC/TOC and OPI parameters indicate a high conversion rate of the original organic matter (Fig. 3, Table 1). In addition, the 'A'/TOC and HC/TOC values of lacustrine limestone in the study area are significantly higher than those of carbonate source rocks in other petroleum-bearing basins (11.6% and 5.0%, respectively), as shown in previous studies (Palacas, 1984) (Fig. 3). In short, although the source rocks, including mudstone and limestone, have relatively low abundances of organic matter, they have a high conversion rate of organic matter. Carbonate rocks with a high conversion rate can ensure that the original organic matters produce considerable oil and gas.

3. The types and maturity of organic matter in the limestone source rocks of the Da'anzhai Member are favorable for hydrocarbon generation. (1) The organic matter types of the limestone and mudstone source rocks are mainly type II. The limestone data also mainly indicate in type II_1 (Fig. 8a). These characteristics can ensure the efficiency of hydrocarbon generation, especially for limestone. (2) The hydrocarbon generation evolution of carbonate source rocks is segmented. The first stage is the thermal depolymerization of biopolymers to provide immature oil, and the second stage is the thermal degradation of kerogen to provide mature oil. The third stage is the release of encapsulated and bound organic matters, which can still provide a certain amount of liquid petroleum at a relatively late stage (Wang et al., 2007). Due to the segmented hydrocarbon generation evolution, high maturity ensures the organic matter conversion rate and hydrocarbon generation scale of carbonate source rocks. (3) The maturity of limestone and mudstone in the Da'anzhai Member is basically the same, showing a high degree of organic matter evolution. The average R_o is 1.14%, and the range is between 0.95% and 1.43% in 14 samples (Fig. 8b). The range of T_{max} values is between 352 °C and 500 °C, with an average value of 447.5 °C (Fig. 8a). In addition, the high maturity and organic matter type can improve the production of light oil and natural gas. Natural gas has an obvious gas mobilization effect on oil development that is helpful for the transport and production of light oil.

4. Under the background of mixed lacustrine deposition, lacustrine carbonate rocks can have a large cumulative thickness in the form of a single layer or an interlayer with mudstone, and can form a complete full-rock hydrocarbon generation system with mudstone. The strong instability of the lake environment leads to

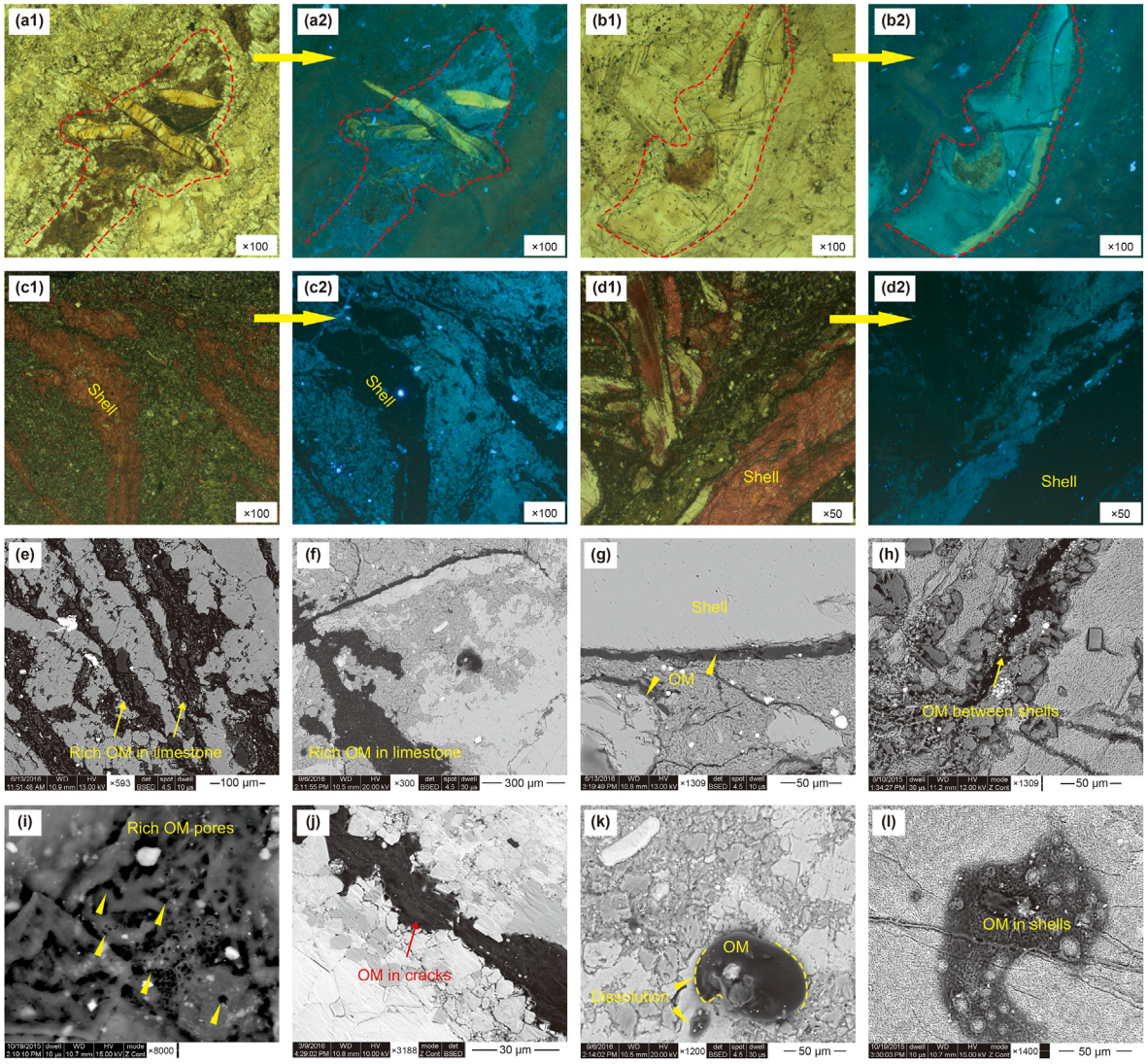

Fig. 7. Microscopic observations of the effectiveness of lacustrine limestone hydrocarbon generation. (a) Obvious fluorescence between the shells. Some shells are also fluorescent (X8, 1740.6 m). (b) Visible fluorescence displayed in and around the shells (X44, 2129.6 m). (c) Strong fluorescence is observable in the limestone matrix (X28, 1952.2 m). (d) Strong fluorescence in the matrix between shells (LQ104X, 3498.6 m). (e) Rich organic matter between shells (S2, 2886.3). (f) Rich organic matter in limestone (S2, 2889.0 m). (g) Organic bands are visible at the edge of the shell (J61, 2664.4 m). (h) Rich organic matter between shells (J61, 2702.6 m). (i) Rich pores are visible in the organic matter, indicating that the organic matter has undergone a strong hydrocarbon generation process (J61, 2669.1 m). (j) Organic bands are visible in the crystalline limestone (X44, 2116.7 m). (k) In situ dissolution of the organic matter indicates that the organic matter has undergone a strong hydrocarbon generation process (S2, 2889.0 m). (l) Organic matter is visible in the shell, and the shell shows an erosion phenomenon, indicating a strong hydrocarbon generation process (G6, 2524.0 m).

Table 4
Low limits of carbonate source rock organic abundance.

NO.	Researcher	TOC, %	NO.	Researcher	TOC, %
1	Ronov (1958)	0.5	11	Li et al. (1999)	0.06–0.2
2	Gehman (1962)	0.2–0.3 (average 0.2)	12	Xia and Dai (2000)	0.5
3	Hunt (1967)	0.29, 0.33 (average 0.3)	13	Zhang et al. (2002)	0.5
4	Zhou and Jia (1974)	0.1	14	Zhang and Wang (2003)	0.5
5	Fu and Liu (1982)	0.1–0.2	15	Qiao (2003)	0.3
6	Palacas (1984)	0.3, 0.5 (average 0.4)	16	Rao et al. (2003)	0.3
7	Tissot and Welte (1984)	0.3	17	Qin et al. (2004)	0.1–0.4
8	Hao (1984)	0.3–0.5	18	Luo et al. (2005)	0.1–0.3
9	Hao and Jia (1989)	0.2	19	Cai et al. (2005)	0.4–0.5
10	Chen (1985)	0.1	20	Wang et al. (2004)	0.3

impure lacustrine carbonate rocks that are mainly composed of interlayered or laminar mudstones and carbonate rocks, and in this case, the cumulative thicknesses of limestone reach 70–100 m. In particular, argillaceous limestone with a relatively high capacity for hydrocarbon generation can reach a large cumulative thickness (50–80 m) and is widely distributed (Fig. 1). Limestone and

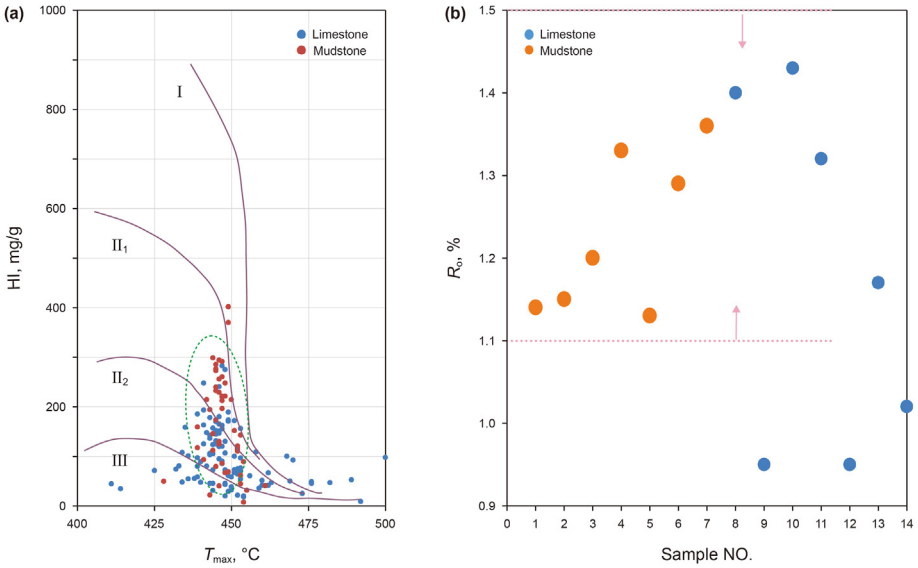

Fig. 8. Type and maturity of organic matter in the Da'anzhai Member. The type of organic matter is mainly II, and the limestone data mainly concentrated in type II_1. The organic maturity of mudstone and limestone is high, R_o values are mainly between 1.1% and 1.5%, and T_{max} is mainly approximately 450 °C.

mudstone can form a thick full-rock system that strongly guarantees the basis for hydrocarbon generation.

In short, the abundance, conversion rate, maturity, types of organic matter and high cumulative thickness can ensure the effectiveness of hydrocarbon generation by limestone.

5.2. Limestone organic matter accumulation in lacustrine mixed sedimentary facies

The shell limestone in the Da'anzhai Member of the central Sichuan Basin occurs in typical lacustrine mixed deposits, and the lacustrine sedimentary facies strongly controls the shell limestone and organic matter enrichment types. Compared with the marine sedimentary environment, the lacustrine sedimentary environment has the following characteristics. (1) The lake is near terrestrial sources with a multisource supply and multideposition center. (2) The deposition cycle is short and developed. (3) The lake wave base is usually shallow, and the wave energy is weaker than that of the marine environment overall (Lima and DE Ros, 2019). (4) The lake water volume is limited, and the environmental regulation ability is weak. As a result of the above characteristics, the carbonate rocks in the study area have typical lacustrine mixed sedimentary characteristics. Three types of mixed sedimentary characteristics can be classified, including in situ mixing, punctuated mixing and facies mixing (Fig. 9) (Ding et al., 2011).

Different sedimentary facies have different mixed deposition and organic matter enrichment types (Fig. 9). (1) The high-energy shelly core corresponds to the area with the highest energy in the shallow lake. A large number of bivalve shell fragments occur in the limestone rock, indicating relatively strong hydrodynamic conditions. A large set of thick shell limestones formed with weak organic matter enrichment. (2) During deposition, the medium to low energy beach edge surrounded the shell beach. Due to the relatively low energy of the water body, the transport capacity and the washing effect were weak in this area. The sediments are mainly composed of a mixture of shells, shell chips, micrite, organic matter and terrestrial inputs. (3) The low-energy lake slope facies were the transition zone between the shell beach and the semideep lake zone and featured a strong reducing environment. The energy of the water body was low, and the transport capacity and washing effect were weaker than those at the beach edge. A large number of shells are visible with the naked eye (Fig. 2a, c). A large number of complete shells oriented along their long axes were observed, indicating in situ burial (Fig. 2g). (4) The semideep and deep lake facies are dominated by black and grey-black shales, and the limestone is dominated by thin interlayers. Argillaceous shell limestone often formed on positive structures with relatively high-energy conditions and high rates of biological deposition. These structures are generally rich in fossils, such as ostracods, pelecypods, charophytes and terrestrial plant fragments, which provide a good basis for organic matter enrichment.

Due to differences in sedimentary facies, the forms and rock types of the shell limestone also differ, and the organic matter enrichment varies markedly (Figs. 1, 9 and 10). The forms of shell limestone mainly include (1) thick shell limestone, (2) thick shell limestone with thin mudstone interlayers, (3) equal-thickness interlayers between shell limestone and mudstone and (4) thin interbedded shell limestone in mudstone (Fig. 10). A good type of limestone source rock is mostly argillaceous limestone with high organic matter contents that formed in a low-energy environment. Organic matter analysis showed that limestone with a high organic matter abundance mostly appears in the form of interlayers (Fig. 10). In the lake slope and semideep lake facies, argillaceous shell limestone mostly coexists with mudstone and appears in the form of interlayers, but the limestone thicknesses and scales are limited. The argillaceous shell limestone from the fore beach to the lake slope is moderately thick and has a relatively high abundance of organic matter, and its effectiveness cannot be ignored (Figs. 9 and 10).

5.3. Limestone organic matter accumulation in lacustrine paleoenvironments

5.3.1. Effects of ***lacustrine paleoenvironments on*** limestone ***organic matter***

A lake lacks environmental regulation abilities and is more susceptible to the impacts of the paleoenvironment and terrestrial inputs than the ocean. The lake sedimentary environment and paleoenvironment strongly control the original composition of sedimentary materials, including minerals and organic matter

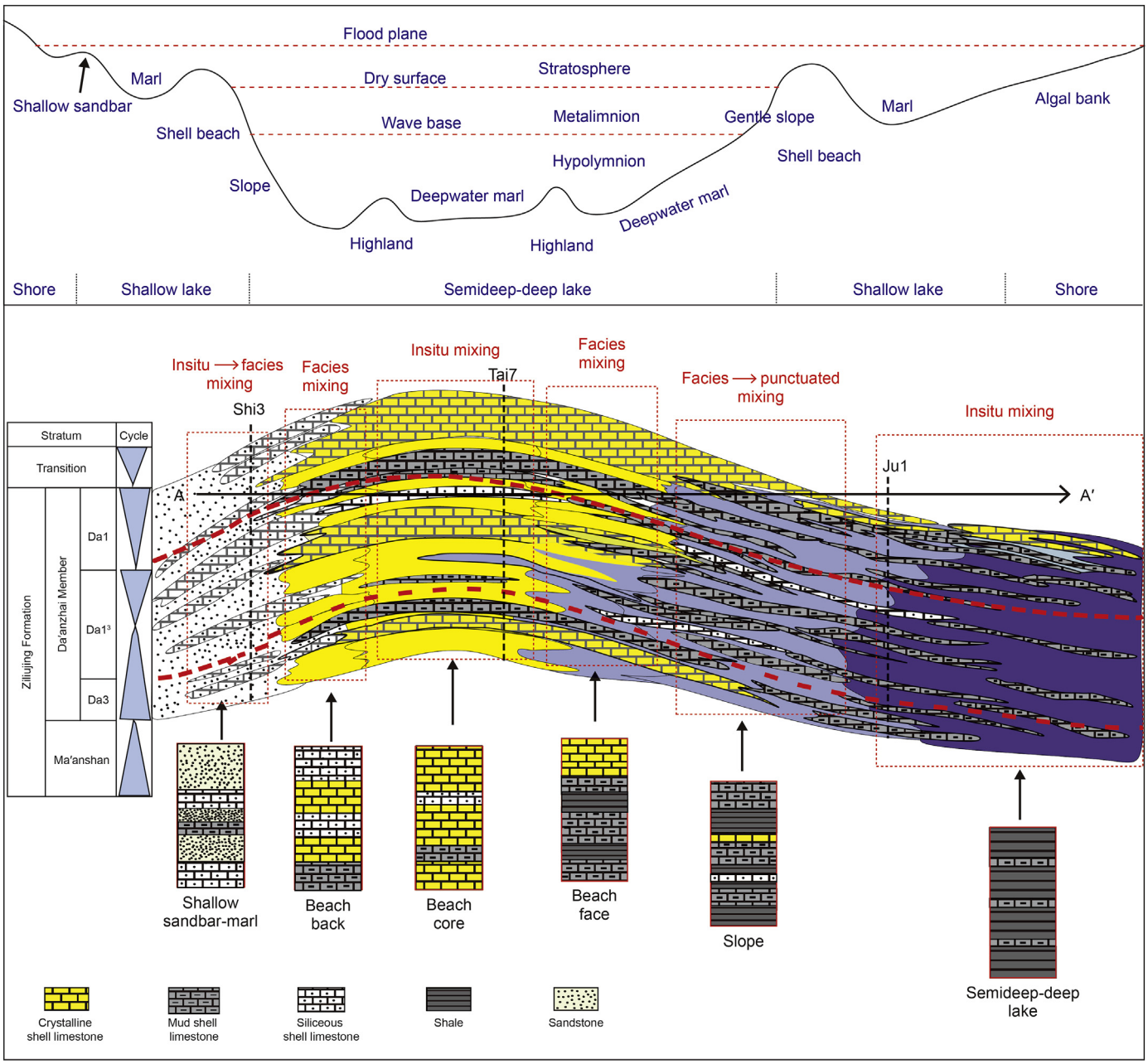

Fig. 9. Lacustrine mixed sedimentary facies and lithologic combinations (profile location is in Fig. 1).

(Wang et al., 1992; Xue et al., 2007; Yu et al., 2022).

Terrestrial inputs. Lacustrine carbonate rocks are generally impure and have abundant terrestrial inputs. Evaporation increases in a long-term closed lake system, and the light ^{16}O and ^{12}C escape preferentially, causing the ^{18}O and ^{13}C contents in the water to increase simultaneously. The carbon and oxygen isotopic compositions of primary carbonate rocks show a covariation trend (Liu et al., 2001; Zhang et al., 2013; Deng et al., 2021). The correlation coefficients between the $\delta^{13}C_{PDB}$ and $\delta^{18}O_{PDB}$ values for the target mudstone and limestone are 0.332 and 0.092, respectively, and they are significantly less than 0.5 (Fig. 4). In addition, the carbon and oxygen isotopes in the study area mostly plot in the terrestrial lacustrine background, and the value range is also closer to the modern open lake background (Fig. 4). These results indicate an open lake type with stable terrestrial inputs and spillover points (Table 2, Fig. 4).

The principles of element migration and sedimentation differentiation can be used to analyze terrestrial inputs (Deng et al., 2021). Al is an important component of terrestrial suspended particles and is basically stable during the transformation of sediments into rocks (Murray et al., 1993). Similarly, elements such as Ti, K and Na are closely related to the terrestrial components in the sediments. These elements must be transported from the source area to enter the lake environment, and their contents can represent terrestrial inputs (Nesbitt and Markovics, 1997). The terrestrial indicator elements (Ti, Al, K and Na) of limestone show a strong positive correlation with the organic matter content. Obviously, the positive correlation is stronger than that between the mudstone and organic matter (Fig. 11).

Biotic productivity. Productivity can strongly control the

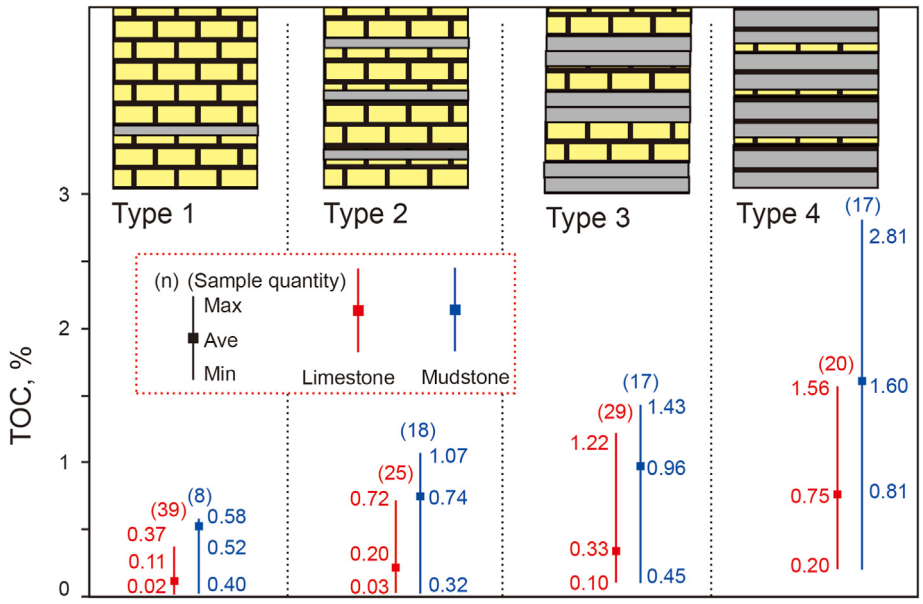

Fig. 10. Existing forms of shell limestone. Type 1. Thick shell limestone; Type 2. Thick shell limestone with thin mudstone interlayers; Type 3. Equal-thickness interlayers between shell limestone and mudstone. Type 4. Thin interbedded shell limestone in mudstone.

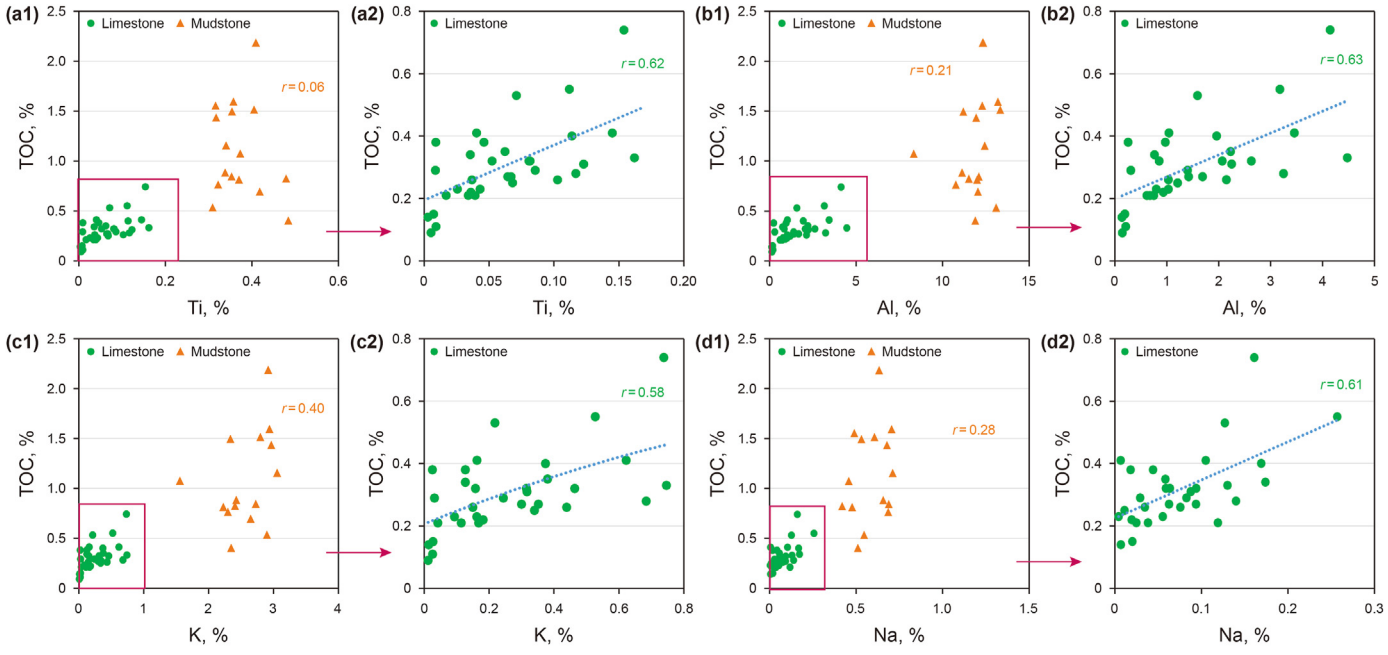

Fig. 11. Relationship between TOC and the indicative elements of terrestrial inputs.

enrichment of organic matter in source rocks. Productivity depends on the richness of nutrients in the surface water (Pedersen and Calvert, 1993). Lacustrine carbonate carbon isotopes are mainly controlled by the dissolved inorganic carbon (DIC) $\delta^{13}C$ of lake water during shell or carbonate formations, and indicate the DIC information in the upper water. DIC is affected by many factors, but the causes of the obvious positive drift can be attributed only to organic matter decomposition by methane bacteria in the diagenesis stage and high lake primary productivity (Li et al., 2000; Garzione et al., 2004; Zhang et al., 2013). The positive drift of carbon isotopes caused by methane bacteria is extremely obvious, and a large number of positive values are greater than 4‰ (Li et al., 2000; Garzione et al., 2004; Zhang et al., 2013). However, most of the $\delta^{13}C_{PDB}$ values in the study area are less than 4‰ (Fig. 4). $\delta^{12}C$ transfers from the surface to the deep part of the lake through plant photosynthesis, and the organic matter produced by photosynthesis is rich in $\delta^{12}C$. When organic matter is decomposed in the bottom water, it releases CO_2 with rich $\delta^{12}C$ to the surrounding water, so the upper water becomes relatively enriched in $\delta^{13}C$ compared to the bottom water (Zhang et al., 2013). When lake phytoplankton flourishes (high primary lake productivity), the $\delta^{13}C$ content of the authigenic carbonate formed in the epilimnion zone increases (Zhang et al., 2013). Therefore, according to the changes in the carbon isotope composition of the lacustrine carbonate rocks,

the biotic productivity can be assessed. The high positive $\delta^{13}C$ values of the lacustrine limestone in the study area mainly indicate high lake primary productivity (Fig. 4). Zn in water is a cofactor of various enzymes. These enzymes, including alcohol dehydrogenase, carbon dehydratase and carboxypeptidase, participate in biological metabolism, which has an important role in the growth of organisms (Anderson and Morel, 1978; Wei, 2012). The positive correlations between the organic matter abundance and the productivity indicator element are strong (Fig. 12a). In lacustrine sedimentary systems, high productivity can guarantee a high accumulation of original organic matter and can result in a high degree of organic matter enrichment under favorable preservation conditions (Fig. 12).

Terrestrial inputs are beneficial to the enrichment of limestone organic matter and can provide the nutrients required by organisms, thereby ensuring high productivity. Terrestrial inputs can also provide large amounts of clay minerals that facilitate the adsorption of organic matter. Appropriate amounts of terrestrial inputs can provide terrestrial nutrients that promote lake biological development, especially during the deposition of carbonate rocks. However, excessive terrestrial inputs can strongly dilute the organic matter in mudstone (Fig. 11).

Paleoclimate. Some elements, including Fe, Mn, Cr, Ni, V, and Co, are relatively enriched under warm and humid climate conditions. In contrast, the strong evaporative environment under drought and hot conditions will cause an increase in the alkalinity of a water body, which in turn causes the precipitation of salt minerals containing Ca, Mg, Sr, Ba, K and Na. Thus, the value of $C = \sum(Fe + Mn + Cr + Ni + V + Co)/\sum(Ca + Mg + Sr + Ba + K + Na)$ can be used as an effective indicator of climate change, and a low value represents drought and hot environment (Zhao et al., 2007; Xu et al., 2019; Yu et al., 2022). The evaporation of lake water in a continental basin during dry periods causes a large amount of Sr deposition in the sediment; thus, low Sr/Cu values indicate warm and humid climates, while high values indicate arid and hot climates (Reheis, 1990; Xu et al., 2019; Yu et al., 2022).

The correlations between the paleoclimate values (C and Sr/Cu) and TOC values of the limestone are strong (Fig. 12). The positive correlation between the C values and the TOC values indicates that a warm, rainy and humid climate was conducive to organic matter enrichment. This positive correlation in the limestone is stronger than that in the mudstone (Fig. 12c). The trend indicated by the Sr/Cu ratio is basically consistent with the trend of C values, and this finding shows that a warm and humid climate was conducive to the enrichment of organic matter in the limestone (Fig. 12b). In short, a warm and humid (rainy) climate ensured sufficient terrestrial inputs, which provided abundant nutrients and thus contributed to high productivity. Excessive terrestrial inputs caused the obvious dilution of organic matter.

Paleoweathering. Under the background of strong weathering, interactions between elements occur. The differentiation between light and heavy rare earth elements (REEs) is notable. The leaching of heavy REEs (HREEs) is strong, especially when the climatic conditions include high temperatures and sufficient water, while light REEs (LREEs) are enriched, resulting in a high degree of differentiation (Kimoto et al., 2006; Stevens and Quinton, 2008; Deng et al., 2021). The REE contents of mudstone are significantly higher than those of limestone, especially crystalline limestone, which has a relatively low REE content. Obvious enrichment in LREEs and depletion of HREEs in the mudstone and limestone are present, and the HREE curves are relatively flat (Fig. 6). These results indicate that the study area experienced strong weathering, and the effect on the enrichment of organic matter cannot be ignored.

In addition, $(La/Sm)_N$, which is the ratio of the normalized values

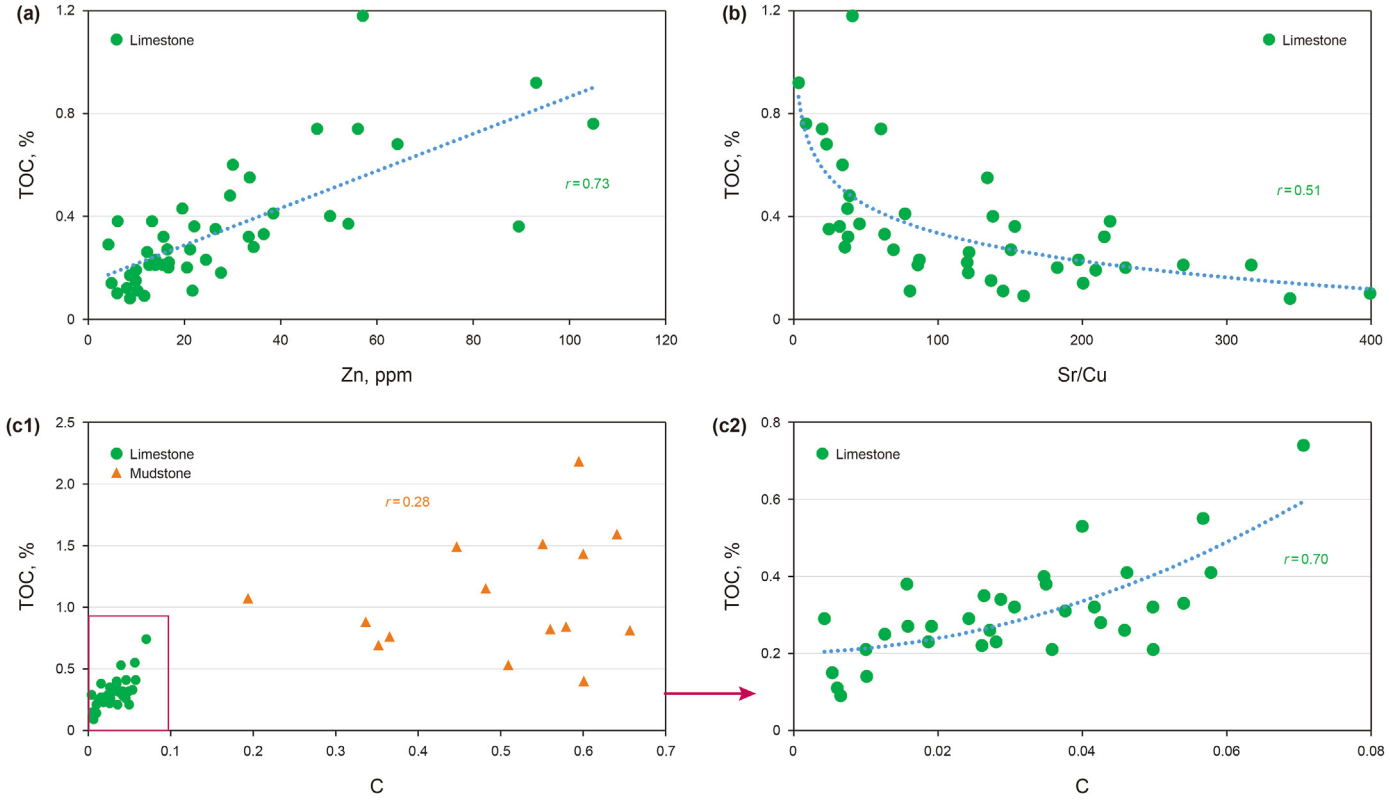

Fig. 12. Relationship between TOC and the indicative elements of biotic productivity and paleoclimate. $C = \sum(Fe + Mn + Cr + Ni + V + Co)/\sum(Ca + Mg + Sr + Ba + K + Na)$.

can effectively represent the degree of differentiation between LREEs. High values represent LREE enrichment and strong weathering (Ross et al., 1995; Ross and Bustin, 2007). Ba/Sr is a good indicator of the weathering degree, and high values indicate a stronger weathering degree (Potter, 1978; Wei et al., 2006). The TOC values are obviously positively correlated with the values of $(La)_N/(Sm)_N$ and Ba/Sr, and the trends in the limestone are clearer than those in the mudstone (Fig. 13). Overall, high weathering rates are associated with warm and rainy climates, resulting in sufficient sources and nutrients that promote productivity, but excessive terrestrial inputs can dilute organic matter.

Hydrodynamics. Hydrodynamics leads to large differences in the growth environments of organisms and affect the growth of lake organisms and the preservation of organic matter. A high Zr content always corresponds to coarse-grained sedimentary rocks, reflecting a high-energy environment. Rb mainly exists in the silicate state in fine particles or light minerals such as clay and mica and easily precipitates in low-energy environments. Thus, the Zr/Rb value is high in relatively volatile high-energy environments (Chen et al., 2006; Dypvik and Harris, 2001). The Zr/Rb values show that the hydrodynamics of the mudstone environment are significantly weaker than those of the limestone environment, and the Zr/Rb values of the mudstone and limestone are negatively correlated with the TOC values (Fig. 13c). A strong hydrodynamic zone represents a turbulent high-oxygen and high-energy environment with a small amount of fine-grained terrestrial inputs, which was harmful to the preservation of organic matter (Fig. 13).

Water depth. An increase in water depth represents a trend of decreasing hydrodynamics and oxygen content. As the lake water deepens, the Sr content significantly increases, and the water depth can be estimated based on the Sr/Ca index. A high Sr/Ca value represents a deep water environment with low oxygen content (Veizer and Demovic, 1974; Jiao et al., 2016). The correlation in Fig. 13d shows that the water depth of the mudstone formation environment was greater than that of the limestone, and this result is consistent with the main formation environments of the limestone and mudstone. The Sr/Ca values of the mudstone and limestone are strongly positively correlated with the TOC values, and the trend is more obvious in the limestone (Fig. 13d). A deep water environment is generally associated with low-oxygen and weak hydrodynamics. This role of water depth in organic matter enrichment is consistent with the roles of hydrodynamics and indicates the importance of reducing conditions for organic matter enrichment.

In summary, the enrichment of organic matter in carbonate rocks is an interactive process involving the paleoenvironment, terrestrial inputs and productivity. Terrestrial inputs are an important factor controlling the accumulation of lacustrine organic matter. Terrestrial inputs can provide abundant nutrients for biological growth, but excessive terrestrial inputs can cause the strong dilution of organic matter. In other words, the promotion effect of terrestrial inputs on the accumulation of organic matter is effective within a certain range. The effects of the paleoclimate and paleoweathering on organic matter are reflected in terrestrial inputs and paleoproductivity; a warm and humid climate is conducive to improving weathering, terrestrial inputs and productivity; and quiet, low-energy and deep conditions result in a reducing environment that is conducive to the preservation of organic matter. Lacustrine carbonate organic matter enrichment should occur in a quiet, low-energy and relatively deep lake zone in a warm and humid climate with an appropriate supply of terrestrial inputs.

However, this favorable paleoenvironment of limestone organic matter formation is not conducive to the deposition of large sets of thick carbonate rocks, and the matching relationship between organic matter enrichment and the carbonate sedimentary scale in lacustrine mixed sedimentary facies should also be considered (Figs. 9 and 10).

5.3.2. Organic matter enrichment models of lacustrine limestone

The lacustrine sedimentary facies and paleoenvironments of the Da'anzhai Member strongly control the shell limestone formation and organic matter enrichment types. The Da'anzhai Member in the central Sichuan Basin experienced a complete lake transgression-maximum flooding surface-lake shrinkage process with a complete low-high-low water level evolution process (Zhang et al., 2013; Lu et al., 2014; Chen et al., 2015; Yang et al.,

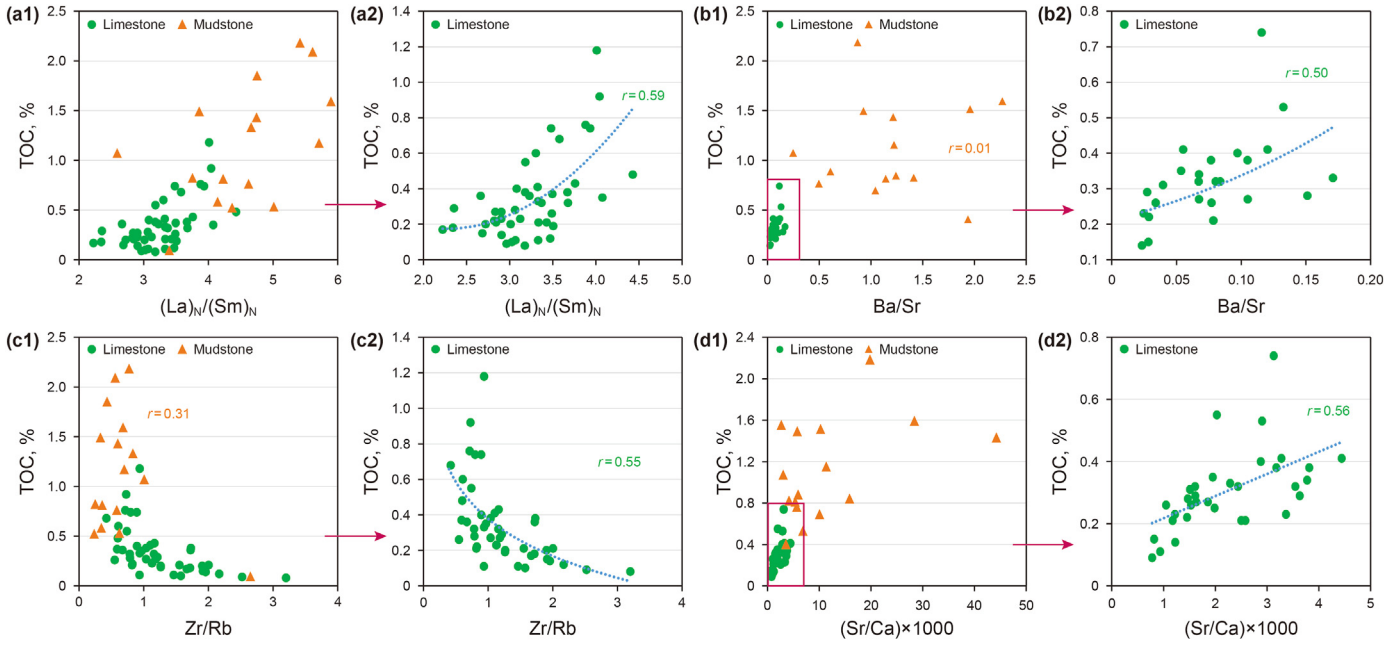

Fig. 13. Relationship between TOC and the indicative elements.

2017; Qiu and He, 2021). The three stages basically correspond to the three sub-members.

The lower part of the Da_3 sub-member is dominated by shell limestone, and the upper part gradually transitions into argillaceous shell limestone and mudstone. With the increase in rainy and humid climate, weathering and water depth, terrestrial inputs gradually increased and reached their peak in the Da_1^3 sub-member (Figs. 1, 9, 14 and 15). From the early to the middle period of the Da_1^3 sub-member, the lithology is dominated by interbedded argillaceous shell limestone and mudstone, showing a trend of gradual deepening of the water body (Figs. 1, 9, 14 and 15). The rocks from the middle stage of Da_1^3 to the early stage of Da_1 are mainly shale intercalated with shell limestone (Figs. 1, 9, 14 and 15). Then, the lacustrine regression gradually progressed in the middle to late stage of the Da_1 sub-member. The upper stage of Da_1 in some shell beach wells shows an increase in siliceous and argillaceous shell limestone, indicating the recession of the lake and increasing terrestrial inputs (Figs. 1 and 14).

Based on the characteristics of the paleoenvironment, terrestrial input, sedimentary facies, and shell limestone formation during different lake basin periods, models of carbonate formation and organic matter enrichment mechanisms were established (Fig. 14).

A: Initial stage of the lake basin with suitable terrestrial inputs. In the early stage of lake development, the lake basin gradually expanded, which involved a transition from low to high water levels (Da_3-Da_1^3). This process coincided with a transition from a hot climate to a warm climate and was accompanied by a gradual increase in terrestrial inputs (Figs. 1, 14 and 15). Initially, a small amount of terrestrial inputs occurred. Due to the jacking effect of the lake on the river, the carrying capacity of the river water was limited. The relatively clear water led to the development of carbonate rocks, but the storage conditions and productivity of the lake for organic matter were limited. In the latter part of this period, the lake basin gradually expanded, and the rainfall and weathering effects increased the terrestrial inputs of the river (Figs. 1, 14 and 15). The abundant nutrients from terrestrial inputs were beneficial for the mass reproduction of organisms. The terrestrial input at this time was conducive to the production of organic matter. Mud-bearing limestones with a large number of shells formed (Figs. 1, 14 and 15).

B: Middle stage of the lake basin with a high water level. The surrounding terrain was flat, and the lake expanded to cover a large

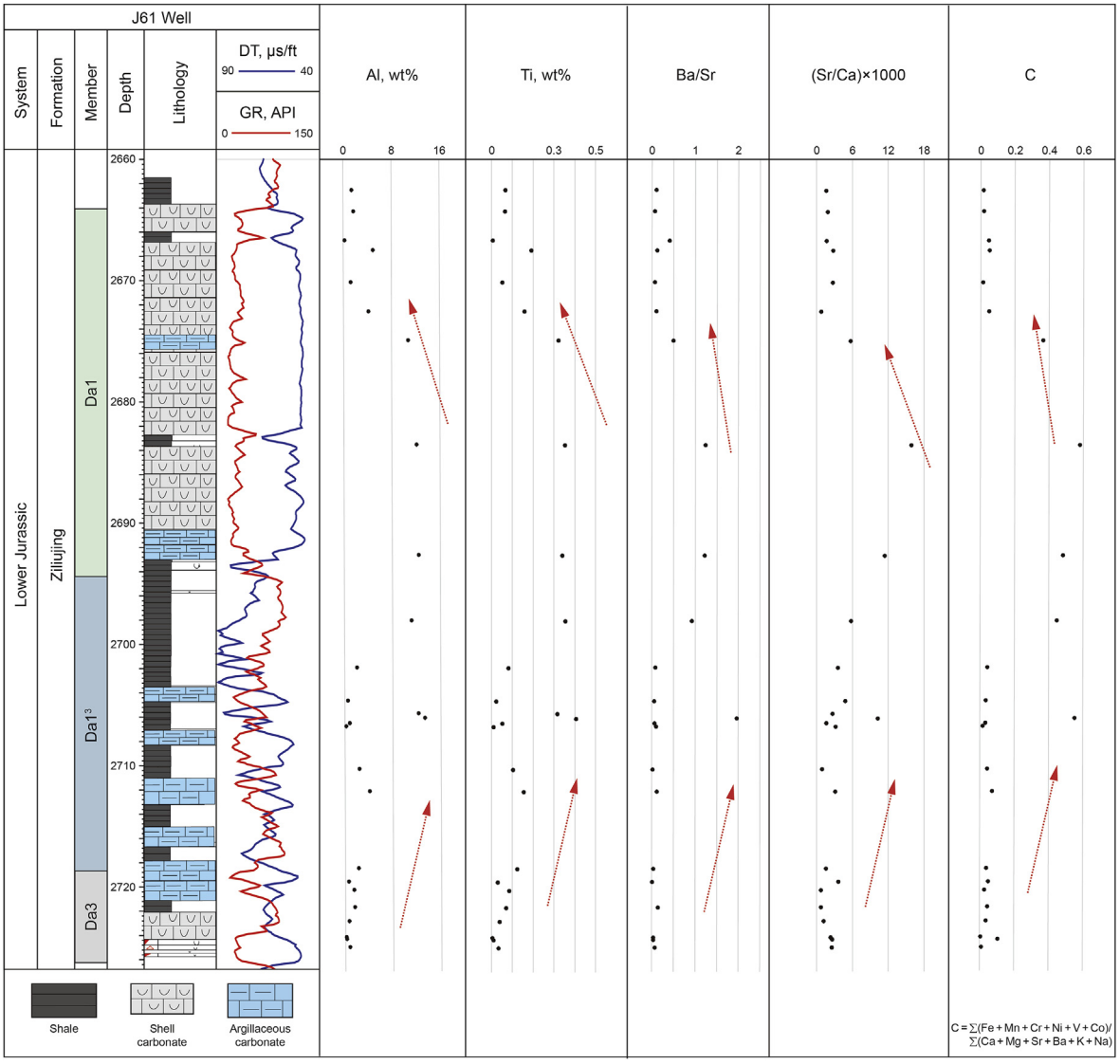

Fig. 14. Characteristics of the lithology and geochemical parameters of the J61well from a stratigraphic perspective.

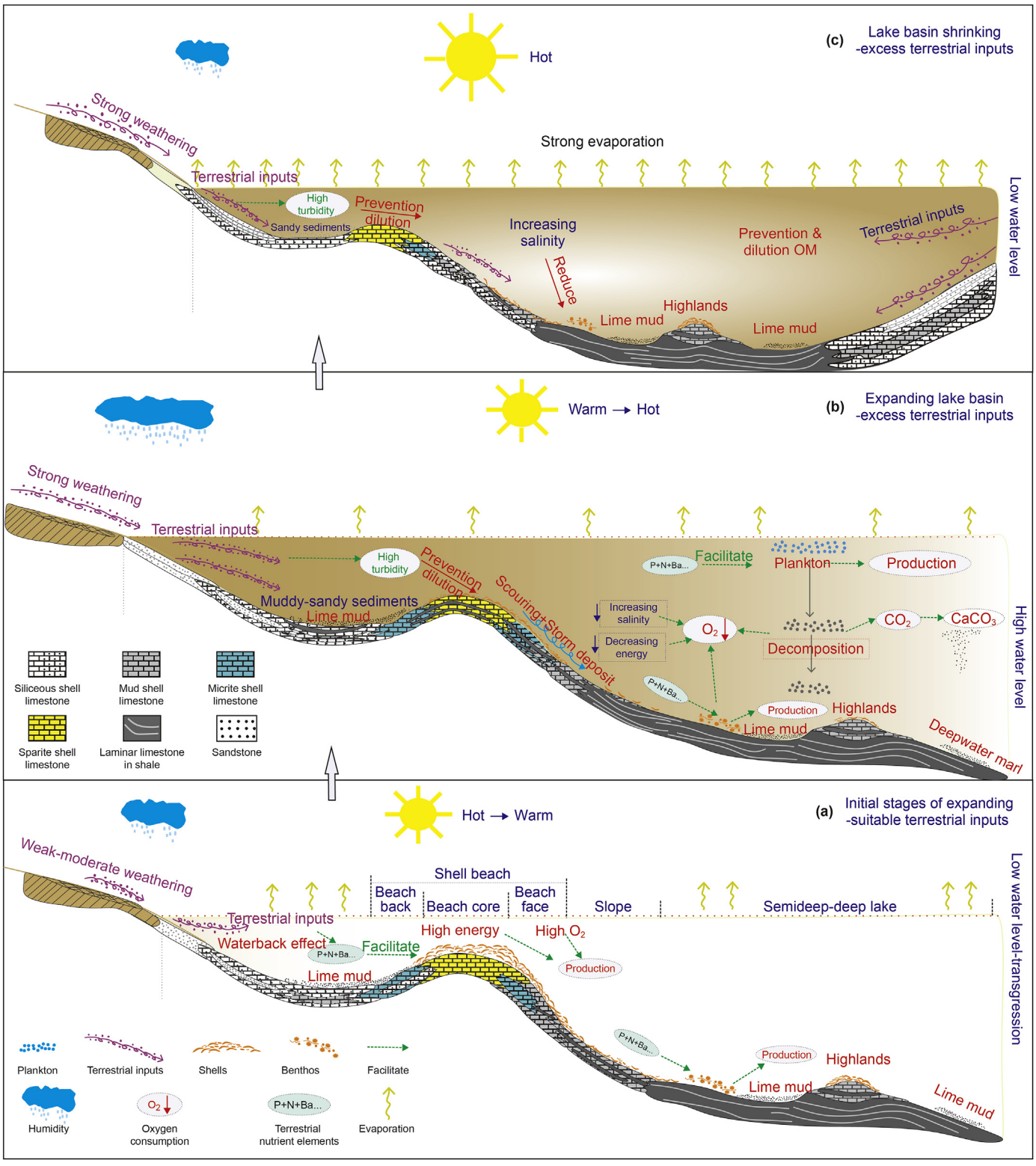

Fig. 15. Lacustrine organic matter enrichment models of limestone in different lake evolution stages. The gradation of color in the basin represents the amount of terrestrial inputs.

area in this stage. The climate was warm to hot with heavy rainfall (Da_1^3-early Da_1). Rivers delivered large amounts of terrestrial inputs containing biological nutrients into the lake. The overall environment of the water body was turbid, which easily formed clastic rocks and mixed rocks, but the environment was not conducive to the formation of carbonate rocks (Figs. 1, 14 and 15). The suitable amount of terrestrial inputs was conducive to the enrichment and preservation of organic matter and resulted in the formation of a thick layer of mudstone source rock. The argillaceous limestone that formed had a relatively high organic matter content. However,

limestone mainly existed in the form of interlayers and played a limited role in organic matter abundance due to its limited thickness and scale (Figs. 1 and 14). With the continued enhancement of terrestrial inputs, the dilution effect was significantly strengthened, which was not conducive to the preservation of organic matter, especially in argillaceous limestone (Figs. 14 and 15).

C: Late stage of the lake basin with suitable/excessive terrestrial inputs. During this process, the climate gradually became drier and hotter, and the area and depth of the lake basin decreased (late Da_1) (Zhang et al., 2013; Yang et al., 2017; Xu et al., 2017). These changes led to a reduction in the environmental regulation capacity of the lake water and easily affected the lake sedimentary environment. At the beginning of this process, terrestrial inputs provided abundant nutrients, which were beneficial to the formation of large sets of thick shell limestone. As the lake basin continued to shrink, the environmental regulation capacity of the lake water was severely reduced. The role of the river began to increase as it carried a large amount of terrestrial inputs. The amount of organic matters began to decrease. Terrestrial inputs and a small amount of marls were the main sediments at the end of this stage (Figs. 1, 14 and 15).

6. Conclusions

1. Although the organic matter content of carbonate rocks is often lower than that of mudstone, the limestone rocks in the Da'anzhai Member can be effective at hydrocarbon generation. (1) The hydrocarbon generation threshold of the limestone source rocks is lower than that of the mudstone source rocks. (2) Limestone rocks can have a higher conversion rate of organic matter than mudstone source rocks. (3) The organic matter types and maturity of limestone source rocks are favorable for hydrocarbon generation. (4) The cumulative thickness of the limestone can reach a relatively high level, and the limestone can form a complete full-rock hydrocarbon generation system with mudstone.
2. The mixed sedimentary environment in the Da'anzhai Member resulted in variable organic matter enrichment types and rock types, and the organic matter in the mud-bearing shell limestone from the forebeach to the lake slope was more effective. The argillaceous shell limestones formed in deep and semideep lakes mostly coexist with mudstone and appear in the form of interlayers, and the limestone deposit thicknesses and scales are limited. The mud-bearing shell limestone deposited from the forebeach to the lake slope is medium-thick with a high organic matter abundance.
3. The Da'anzhai Member records a complete lake expansion-shrinkage evolution process, and organic matter enrichment in the limestone mainly involves the interaction of the paleoenvironments and terrestrial inputs. Terrestrial inputs can provide abundant nutrients for biological growth, but excessive terrestrial inputs can cause the dilution of organic matter. A favorable enrichment environment for limestone organic matter should comprise a quiet, low-energy and deep lake zone in a warm and humid climate with an appropriate supply of terrestrial inputs, but it is unfavorable for the limestone deposit thicknesses and scales.

Acknowledgments

Our study is supported by the National Natural Science Foundation of China (Grants 41902131 and 41821002 and 4169130014). The authors also sincerely appreciate support from the PetroChina Research Institute of Petroleum Exploration and Development, and the Sichuan Basin Research Center of PetroChina Southwest Oil and Gas Field Company.

References

Anderson, M.A., Morel, F.M.M., 1978. Growth limitation of a coastal diatom by low zinc ion activity. Nature 276, 70–71. https://doi.org/10.1038/276070a0.
Beckmann, B., Flögel, S., Hofmann, P., et al., 2005. Orbital forcing of Cretaceous river discharge in tropical Africa and ocean response. Nature 437 (7056), 241–244. https://doi.org/10.1038/nature03976.
Cai, X.Y., Wei, B.D., Zhao, P.R., 2005. Characteristics of the marine hydrocar-bon source rocks in South China. Nat. Gas. Ind. 25 (3), 20–22. https://doi.org/10.1360/gs050303 (in Chinese).
Chen, P.J., 1985. Comment on several topics in the geochemistry carbonate source rock. Petrol. Geol. Exp. 7 (1), 3–12. https://doi.org/10.11781/sysydz198501003 (in Chinese).
Chen, J., Chen, Y., Liu, L.W., et al., 2006. Zr/Rb ratio in the Chinese loess s-equences and its implication for changes in the East Asian winter monsoon strength. Geochem. Cosmochim. Acta 70, 1471–1482. https://doi.org/10.1016/j.gca.2005.11.029.
Chen, S., Zhang, H., Lu, J., et al., 2015. Controlling factors of Jurassic Da'an-zhai Member tight oil accumulation and high production in central Sichuan Basin, SW China. Petrol. Explor. Dev. 42 (2), 206–214. https://doi.org/10.1016/S1876-3804(15)30007-0 (in Chinese).
Deaf, A.S., El Soughier, M.I., Gentzis, T., et al., 2021. Hydrocarbon source rock potential of the Lower Eocene carbonates from the Abu Darag sub-basin, Gulf of Suez, Egypt: integrated organic geochemical and petrographic analyses. Mar. Petrol. Geol. 132, 105235. https://doi.org/10.1016/j.marpetgeo.2021.105235.
Deng, S., Wang, Y., Hu, Y., et al., 2013. Integrated petrophysical log character-ization for tight carbonate reservoir effectiveness: a case study from the -Longgang area, Sichuan Basin, China. Petrol. Sci. 10 (3), 336–346. https://doi.org/10.1007/s12182-013-0282-5.
Deng, Q., Wang, H., Wei, Z., et al., 2021. Different accumulation mechanisms of organic matter in Cambrian sedimentary successions in the western and northeastern margins of the Tarim Basin, NW China. J. Asian Earth Sci. 207, 104660. https://doi.org/10.1016/j.jseaes.2020.104660.
Di, Y., Li, Z., Feng, F., et al., 2013. Mixing of lacustrine siliciclastic-carbonate sediments and its significance for tight oil exploration in the daanzhai member, ziliujing formation, lower jurassic, in longgang area, central Sichuan Basin. Geol. Rev. 59 (2), 389–400. https://doi.org/10.16509/j.georeview.2013.02.013 (in Chinese).
Ding, W.L., Li, C., Su, A.G., et al., 2011. Study on the comprehensive geochemical cross section of Mesozoic marine source rocks and prediction of favorable hydrocarbon generation area in Qiangtan basin. Tibeta. Acta Petrol. Sin. 27 (3), 878–896. https://doi.org/10.1007/s12182-011-0118-0 (in Chinese).
Dypvik, H., Harris, N.B., 2001. Geochemical facies analysis of fine-grained siliciclastics using Th/U, Zr/Rb and (Zr+Rb)/Sr ratios. Chem. Geol. 181, 131–146. https://doi.org/10.1016/S0009-2541(01)00278-9.
Fu, J.M., Liu, D.H., 1982. Some characteristics of the evolution of organic m-atter in carbonate formation. Acta Petrol. Sin. 3 (1), 1–9. https://doi.org/10.1016/0079-1946(79)90087-9 (in Chinese).
Gao, G., Yang, S., Ren, J., et al., 2018. Geochemistry and depositional conditions of the carbonate-bearing lacustrine source rocks: a case study from the Early Permian Fengcheng Formation of Well FN7 in the northwestern Junggar Basin. J. Petrol. Sci. Eng. 162, 407–418. https://doi.org/10.1016/j.petrol.2017.12.065.
Garzione, C.N., Dettman, D.L., Horton, B.K., 2004. Carbonate oxygen isotope paleoaltimetry: evaluating the effect of diagenesis on paleoelevation estimates for the Tibetan plateau. Palaeogeogr. Palaeocl. 212 (1–2), 119–140. https://doi.org/10.1016/j.palaeo.2004.05.020.
Gehman, H.M., 1962. Organic matter in limestone. Geochem. Cosmochim. Acta 26, 885–894. https://doi.org/10.1016/0016-7037(62)90118-7.
Guo, P., Liu, C., Gibert, L., et al., 2020. How to find high-quality petroleum source rocks in saline lacustrine basins: a case study from the Cenozoic Qaidam Basin, NW China. Mar. Petrol. Geol. 111, 603–623. https://doi.org/10.1016/j.marpetgeo.2019.08.050.
Han, K., Wang, Y., Zha, Q., 2015. Exploration potential and targets of Jurassic system in central Sichuan. Oil Forum (6), 51–57. https://doi.org/10.3969/j.issn.1002-302x.2015.06.011 (in Chinese).
Hao, S.S., 1984. Richness of organic matter and its evolutional characteristics in carbonate source rocks. Petrol. Geol. Exp. 6 (1), 17–24. https://doi.org/10.11781/sysydz198401067 (in Chinese).
Hao, S.S., Jia, Z.Y., 1989. The Formation and Distribution of Oil and Gases in Carbonate Rocks. Petroleum Industry Press, Beijing, pp. 89–102 (in Chinese).
Hao, F., Zhou, X., Zhu, Y., et al., 2011. Lacustrine source rock deposition in response to co-evolution of environments and organisms controlled by tectonic subsidence and climate, Bohai Bay Basin. China. Org. Geochem. 42 (4), 323–339. https://doi.org/10.1016/j.orggeochem.2011.01.010.
Harris, N.B., Freeman, K.H., Pancost, R.D., et al., 2004. The character and origin of lacustrine source rocks in the Lower Cretaceous synrift section, Congo Basin, west Africa. AAPG Bull. 88 (8), 1163–1184. https://doi.org/10.1306/02260403069.
Hu, D., Wang, L., Zhang, H., et al., 2021. Discovery of carbonate source rock gas reservoir and its petroleum geological implications: a case study of the gas reservoir in the first member of Middle Permian Maokou Formation in the Fuling area, Sichuan Basin. Nat. Gas. Ind. B 8 (1), 13–23. https://doi.org/10.1016/j.ngib.2020.07.001 (in Chinese).
Hunt, J.M., 1967. Chapter 7 the origin of petroleum in carbonate rocksk. Dev.

Sedimentol. 9, 225–251. https://doi.org/10.1016/j.jseaes.2019.01.038.
Jiang, S., Tang, X., Cai, D., et al., 2016. Comparison of marine, transitional, and lacustrine shales: a case study from the sichuan basin in China. J. Petrol. Sci. Eng. 150, 334–347. https://doi.org/10.1016/j.petrol.2016.12.014.
Jiao, P., Guo, J., Zhang, X., et al., 2016. Element geochemistry of the Neogene Zhujiang formation mudstones in Lufeng depression, Pearl River Mouth basin and its geological implication. J. Cent. South Univ. (Sci. Tech.). 47 (7), 2347–2356. https://doi.org/10.11817/j.issn.1672-7207.2016.07.024 (in Chinese).
Kaufman, A.J., Jacobsen, S.B., Knoll, A.H., 1993. The Vendian record of Sr a-nd C isotopic variations in seawater: implications for tectonics and paleoc-limate. Earth Planet Sci. Lett. 120 (3–4), 409–430. https://doi.org/10.1016/0012-821X(93)90254-7.
Ke, C., Li, S., Greenwood, P., et al., 2022. Maturity and depositional controls on compound-specific sulfur isotope values of saline lacustrine source rocks in the north Dongpu Depression, Bohai Bay Basin. J. Petrol. Sci. Eng. 212, 110286. https://doi.org/10.1016/j.petrol.2022.110286.
Kennedy, M.J., Pevear, D.R., Hill, R.J., 2002. Mineral surface control of organic carbon in black shale. Science 295, 657–660. https://doi.org/10.1126/scienc-e.1066611.
Kietzmann, D.A., Palma, R.M., Riccardi, A.C., et al., 2014. Sedimentology and sequence stratigraphy of a Tithonian-Valanginian carbonate ramp (Vaca Muerta Formation): a misunderstood exceptional source rock in the Southern Mendoza area of the Neuquén Basin. Argentina. Sediment. Geol. 302, 64–86. https://doi.org/10.1016/j.sedgeo.2014.01.002.
Kimoto, A., Nearing, M.A., Shipitalo, M.J., et al., 2006. Multi-year tracking of sediment sources in a small agricultural watershed using rare earth elements. Earth Surf. Process. Landforms 31 (14), 1763–1774. https://doi.org/10.1002/esp.1355.
Klemme, H.D., Ulmishek, G.F., 1991. Effective petroleum source rocks of the world: stratigraphic distribution and controlling depositional factors. AAPG bulletin 75 (12), 1809–1851. https://doi.org/10.1306/0C9B2A47-1710-11D7-8645000102C1865D.
Koch, G., Prtoljan, B., Husinec, A., et al., 2017. Palynofacies and paleoenvironment of the Upper Jurassic mud-supported carbonates, southern Croatia: preliminary evaluation of the hydrocarbon source rock potential. Mar. Petrol. Geol. 80, 243–253. https://doi.org/10.1016/j.marpetgeo.2016.12.006.
Lawal, L.O., Adebayo, A.R., Mahmoud, M., et al., 2021. Thermal maturation, mineral catalysis, and gas generation kinetics of carbonate source rock. J. Nat. Gas Sci. Eng. 92, 104003. https://doi.org/10.1016/j.jngse.2021.104003.
Li, Y.J., Chen, Y.C., Yang, Y.C., 1999. Source rock evaluation and characteristics of hydrocarbon generation from Lower Paleozoic carbonate in Ordos basin. Oil Gas Geol. 20 (4), 349–353. https://doi.org/10.11743/ogg19990418 (in Chinese).
Li, H.C., Bischoff, J.L., Ku, T.L., 2000. Climate variability in East-Central California during the past 1000 years reflected by high-resolution geochemical and isotopic records from Owens Lake sediments. Quat. Res. 54 (2), 189–197. https://doi.org/10.1006/qres.2000.2163.
Lima, B.E.M., DE Ros, L.F., 2019. Deposition, diagenetic and hydrothermal processes in the Aptian Pre-Salt lacustrine carbonate reservoirs of the northern Campos Basin, offshore Brazil. Sediment. Geol. 383, 55–81. https://doi.org/10.1016/j.sedgeo.2019.01.006.
Liu, C.L., Zhao, Q.H., Wang, P.X., 2001. Correlation between carbon and oxygen isotopic ratios of lacustrine carbonates and types of oil-producing paleolakes. Geochemistry 30 (4), 363–367. https://doi.org/10.19700/j.0379-1726.2001.04.009.
Liu, B., Mastalerz, M., Schieber, J., 2021. SEM petrography of dispersed organic matter in black shales: a review. Earth Sci. Rev. https://doi.org/10.1016/j.earscirev.2021.103874, 103874.
Lu, B.X., Zheng, R.C., Liang, X.W., et al., 2014. Characteristics analysis of Da'anzhai shale gas (oil) reservoirs in eastern Sichuan Basin. Chin. Geol. 41, 1387–1398. https://doi.org/10.3969/j.issn.1000-3657.2014.04.028 (in Chinese).
Luo, X.Y., Meng, Y.L., Chen, Y.L., et al., 2005. An evaluation of Ordovician hydrocarbon source rock and its lower limit of organic abundance in Dagang area, Huanghua depression. China Offshore Oil Gas 17 (5), 303–307. https://doi.org/10.3969/j.issn.1673-1506.2005.05.003 (in Chinese).
Murray, R.W., Leinen, M., Isern, A.R., 1993. Biogenic flux of Al to sediment in the central equatorial Pacific ocean: evidence for increased productivity during glacial periods. Paleoceanogr. Paleoclimatol. 8, 651–670. https://doi.org/10.1029/93PA02195.
Nesbitt, H.W., Markovics, G., 1997. Weathering of granodioritic crust, long-term storage of elements in weathering profiles, and petrogenesis of siliciclastic sediments. Geochem. Cosmochim. Acta 61 (8), 1653–1670. https://doi.org/10.1016/S0016-7037(97)00031-8.
Palacas, J.G., 1984. Petroleum geochemistry and source rock potential of carbonate rocks. AAPG Stud. Geol. 71–96, 127–134. https://doi.org/10.1306/St18443.
Pedersen, T.F., Calvert, S.E., 1993. Anoxia vs. productivity: what controls the -formation of organic-carbon-rich sediments and sedimentary rock? AAPG Bull. 74, 454–466. https://doi.org/10.1306/0C9B232B-1710-11D7-8645000102C1865D.
Pinto, F.G., Junior, R.E., Saint'Pierre, T.D., 2012. Sample preparation for determination of rare earth elements in geological samples by ICP-MS: a critical review. Analytical letters 45 (12), 1537–1556. https://doi.org/10.1080/00032719.2012.677778.
Potter, P.E., 1978. Petrology and chemistry of modern big river sands. J. Geol. 86, 423–449. https://doi.org/10.1086/649711.
Qiao, G.L., 2003. An analysis on hydrocarbon generation potential in Tazhong uplift and Neighboring Tanggubazi depression. Henan Petrol 17 (5), 4–9. https://doi.org/10.3969/j.issn.1673-8217.2003.05.002 (in Chinese).
Qin, J.Z., Liu, B.Q., Guo, J.Y., 2004. Discussion on the evaluation standards of carbonate source rocks. Petrol. Geol. Exp. 26 (3), 281–286. https://doi.org/10.11781/sysydz200403281.
Qiu, Z., He, J., 2021. Depositional environment changes and organic matter accumulation of Pliensbachian-Toarcian lacustrine shales in the Sichuan basin, SW China. J. Asian Earth Sci. 232, 105035. https://doi.org/10.1016/j.jseaes.2021.105035.
Qiu, L., Yan, D.P., Tang, S.L., et al., 2016. Mesozoic geology of southwestern China: Indosinian foreland overthrusting and subsequent deformation. J. Asian Earth Sci. 122, 91–105. https://doi.org/10.1016/j.jseaes.2016.03.006.
Rao, D., Zhang, P.A., Qiu, Y.Y., 2003. Discussion on lower limit of content of organic matters for effective source rocks. Petrol. Geol. Exp. 25, 578–581. https://doi.org/10.1039/b804718a (in Chinese).
Reheis, M.C., 1990. Influence of climate and eolian dust on the major-element chemistry and clay mineralogy of soils in the northern Bighorn Basin, USA. Catena 17 (3), 219–248. https://doi.org/10.1016/0341-8162(90)90018-9.
Ronov, A.B., 1958. Organic carbonic sedimentary rocks (in relation to the pres-ence of petroleum). Geochem. (Tokyo. 1967) 5, 497–507. https://doi.org/10.1111/j.1747-5457.1983.tb00262.x.
Ross, D.J.K., Bustin, R.M., 2007. Shale gas potential of the lower jurassic gordondale member, northeastern British columbia, Canada. Bull. Can. Petrol. Geol. 55, 51–75. https://doi.org/10.2113/gscpgbull.55.1.51.
Ross, D.J.K., Bustin, R.M., 2009. Investigating the use of sedimentary geochemical proxies for paleoenvironment interpretation of thermally mature organic-rich strata: examples from the Devoniane-Mississippian shales. West. Can. Sediment. Basin. Chem. Geol. 260, 1–19. https://doi.org/10.1016/j.chemgeo.2008.10.027.
Ross, G.R., Guevara, S.R., Arribere, M.A., 1995. Rare earth geochemistry in sediments of the Upper Manso river basin, Rio Negro, Argentina. Earth Planet Sci. Lett. 133 (1–2), 47–57. https://doi.org/10.1016/0012-821X(95)00060-.
Ruhl, M., Deenen, M.H.L., Abels, H.A., et al., 2010. Astronomical constraints on the duration of the early Jurassic Hettangian stage and recovery rates following the end-Triassic mass extinction (St Audrie's Bay/East Quantoxhead, UK). Earth Planet Sci. Lett. 295 (1–2), 262–276. https://doi.org/10.1016/j.epsl.2010.04.008.
Shanks, A.L., Trent, J.D., 1980. Marine snow: sinking rates and potential role -in vertical flux. Deep-Sea Res. PT. A. 27 (2), 137–143. https://doi.org/10.1016/0198-0149(80)90092-8.
Shi, J., Jin, Z., Liu, Q., Huang, Z., 2020. Lithofacies classification and origin of the eocene lacustrine fine-grained sedimentary rocks in the Jiyang depression, bohai bay basin, eastern China. J. Asian Earth Sci. 194, 104002. https://doi.org/10.1016/j.jseaes.2019.104002.
Stank, C.V., Esteves, F.R., Martins, C.C., et al., 1992. The Linguado, Carapeba, Vermelho, and Marimba giant oil fields, Campos basin, offshore Brazil. AAPG Bull. 74. https://doi.org/10.1306/M54555C9.
Stevens, C.J., Quinton, J.N., 2008. Investigating source areas of eroded sediments transported in concentrated overland flow using rare earth element tracers. Catena 74 (1), 31–36. https://doi.org/10.1016/j.catena.2008.01.002.
Talbot, M.R., 1990. A review of the palaeohydrological interpretation of carbon and oxygen stable isotopic ratios in primary carbonates. Chem. Geol. 80, 261–279. https://doi.org/10.1016/0168-9622(90)90009-2.
Talbot, M.R., 1994. Paleohydrology of the late miocene ridge basin lake, cali-fornia. Geol. Soc. Am. Bull. 106, 1121–1129. https://doi.org/10.1130/0016-7606(1994)106<1121:POTLMR>2.3.CO;2.
Tissot, B.P., Welte, D.H., 1984. Petroleum Formation and Occurrence (Second R Evised and Enlarged Edition). SpringerVerlag Berlin Heidelberg, New York, pp. 160–198.
Veizer, J., Demovic, R., 1974. Strontium as a tool for facies analysis. Sediment. Petrology 44 (1), 93–115. https://doi.org/10.1306/74D72991-2B21-11D7-8648000102C1865D.
Veizer, J., Ala, D., Azmy, K., 1999. 87Sr/86Sr, δ13C and δ18O evolution of Phanerozoic seawater. Chem. Geol. 161, 59–88. https://doi.org/10.1016/S0009-2541(99)00081-9.
Wang, Y., Zhou, S., Zhang, X., 1992. Lake Carbonate Rock in China. China Mining University Press, Xuzhou, pp. 1–123 (in Chinese).
Wang, Z.Y., Zhao, W.Z., Wang, Y.P., 2004. Evaluation criteria for gas source rocks of mari-ne carbonate in China. Prog. Nat. Sci. 15, 810–817. https://doi.org/10.1080/10020070512331342960.
Wang, G., Wang, T., Zhang, L., 2007. Hydrocarbon-generation characteristics for lacustrine carbonate source rocks in Bonan Sag of Jiyang Depression. Acta Petrol. Sin. 28 (2), 62–68. https://doi.org/10.7623/syxb200206011.
Wedepohl, K.H., 1971. Environmental influences on the chemical composition of shales and clays. Phys. Chem. Earth 8, 305–333. https://doi.org/10.1016/0079-1946(71)90020-6.
Wei, H., 2012. Productivity and redox proxies of palaeo-oceans: an overview of elementary geochemistry. Sediment. Geol. Tethyan Geol. 32 (2), 76–88. https://doi.org/10.3969/j.issn.1009-3850.2012.02.012 (in Chinese).
Wei, G.J., Li, X.H., Liu, Y., 2006. Geochemical record of chemical weathering and monsoon climate change since the early miocene in the south China sea. Paleoceanography 21 (4), 1–11. https://doi.org/10.1029/2006PA001300.
Xia, X.Y., Dai, J.X., 2000. A critical review on the evaluation of hydrocarbon potential of marine carbonate rocks in China. Acta Petrol. Sin. 21 (4), 36–41. https://doi.org/10.7623/syxb200004007 (in Chinese).
Xia, L.W., Cao, J., Wang, M., et al., 2019. A review of carbonates as hydrocarbon source rocks: basic geochemistry and oil-gas generation. Petrol. Sci. 16 (4), 713–728. https://link.springer.com/article/10.1007/s12182-019-0343-5.
Xing, L.T., Xu, L., Zhang, P.Z., et al., 2022. Organic geochemical characteri-stics of

saline lacustrine source rocks: a case study from the yingxi Ar-ea, Qaidam Basin, China. Geochem. Int. 60 (1), 92–108. https://doi.org/10.1134/S0016702921150015.

Xu, Q., Liu, B., Ma, Y., et al., 2017. Controlling factors and dynamical formation models of lacustrine organic matter accumulation for the Jurassic Da'anzhai Member in the central Sichuan Basin, southwestern China. Mar. Petrol. Geol. 86, 1391–1405. https://doi.org/10.1016/j.marpetgeo.2017.07.014.

Xu, Q., Ma, Y., Liu, B., et al., 2019. Characteristics and control mechanism of nano-scale pores in lacustrine tight carbonates: examples from the Jurassic Da'anzhai Member in the central Sichuan Basin, China. J. Asian Earth Sci. 178, 156–172. https://doi.org/10.1016/j.jseaes.2018.05.009.

Xu, Q., Hao, F., Ma, Y., et al., 2020. Effects of the matrix on the oil production of supertight limestone in a lacustrine mixed sedimentary environment: the case of the Jurassic Da'anzhai member in the central Sichuan Basin, China. Mar. Petrol. Geol. 121, 104583. https://doi.org/10.1016/j.marpetgeo.2020.104583.

Xue, H.T., Wang, H.H., Lu, S.F., 2007. Standard related to TOC classification evaluation of carbonate oil source rocks. Acta Sedimentol. Sin. 25 (5), 782–785. https://doi.org/10.3969/j.issn.1000-0550.2007.05.019 (in Chinese).

Yang, G., Huang, D., Huang, P., et al., 2017. Control factors of high and stab-le production of Jurassic Da'anzhai Member tight oil in central Sichuan B-asin, SW China. Petrol. Explor. Dev. 44 (5), 866–875. https://doi.org/10.1016/S1876-3804(17)30098-8.

Yu, W., Tian, J., Wang, F., et al., 2022. Sedimentary environment and organic matter enrichment of black mudstones from the upper Triassic Chang-7 member in the Ordos Basin, Northern China. J. Asian Earth Sci. 224, 105009. https://doi.org/10.1016/j.jseaes.2021.105009.

Zachos, J., Pagini, M., Sloan, L., 2001. Trends, rhythms, and aberrations in gl-obal climate 65 Ma to present. Science 292, 686–693. https://doi.org/10.1126/science.1059412.

Zhang, K., Wang, D.R., 2003. Some thoughts on petroleum exploration in marine sedimentary basins of China. Petrol. Explor. Dev. 30 (2), 9–16. https://doi.org/10.3321/j.issn:1000-0747.2003.02.002 (in Chinese).

Zhang, S.C., Liang, D.G., Zhang, D.J., 2002. Evaluation criteria for Paleozoic effective hydroncarbon source rocks. Petrol. Explor. Dev. 29 (2), 8–12. https://doi.org/10.3321/j.issn:1000-0747.2002.02.002.

Zhang, W., Li, Z.W., Feng, F., et al., 2013. Carbon and oxygen isotopic composition of lacustrine carbonate rocks of the Lower-Middle Jurassic in NE part of central Sichuan Province and their palaeoenvironmental significance. J. Palaeogeogr. 15 (2), 247–259. https://doi.org/10.7605/gdlxb.2013.02.021.

Zhang, S., Wang, X., Hammarlund, E.U., et al., 2015. Orbital forcing of climate 1.4 billion years ago. P. Natl. Acad. Sci. USA. 112 (12), 1406–1413. https://doi.org/10.1073/pnas.1502239112.

Zhao, Z.Y., Zhao, J.H., Wang, H.J., et al., 2007. Distribution characteristics and applications of trace elements in Junggar Basin. Nat. Gas Explor. Dev. 30 (2), 30–32. https://doi.org/10.3969/j.issn.1673-3177.2007.02.007 (in Chinese).

Zhao, Y., Cai, J.G., Lei, T.Z., et al., 2018. A geochemical investigation of the free and carbonate-bound organic matter in the clay-sized fraction of argillaceous source rocks and its significance for biogenic interpretation. Petrol. Sci. 15 (4), 681–694. https://link.springer.com/article/10.1007/s12182-018-0257-7.

Zhou, J., 2018. Research on the Heterogeneity of the Chang 9 Reservoir in the H224 District of the JY Oilfield in Ordos Basin. Xi'an Shiyou University, Xi'an, pp. 1–49 (in Chinese).

Zhou, Z.Y., Jia, R.F., 1974. Organic Geochemical and petrological characteristics of carbonate rocks as a source rock for petroleum. Geochem. (Tokyo. 1967) 3 (4), 278–296. https://doi.org/10.19700/j.0379-1726.1974.04.007 (in Chinese).

Zhu, G.Y., Jin, Q., 2002. Study on source rock heterogeneity- a case of Niu-37 well in dongying depression. Acta Petrol. Sin. 23 (5), 34–39. https://doi.org/10.7623/syxb200205007 (in Chinese).

Zonneveld, K.A., Versteegh, G.J., Kasten, S., et al., 2010. Selective preservation of organic matter in marine environments; processes and impact on the sedimentary record. Biogeosciences 7 (2), 483–511. https://doi.org/10.5194/bg-7-483-2010.